

THE ALPHA MAGNETIC SPECTROMETER (AMS) EXPERIMENT

■ SAMUEL TING

Massachusetts Institute of Technology

Presented at the International Symposium on Subnuclear Physics: Past, Present and Future, November 1, 2011

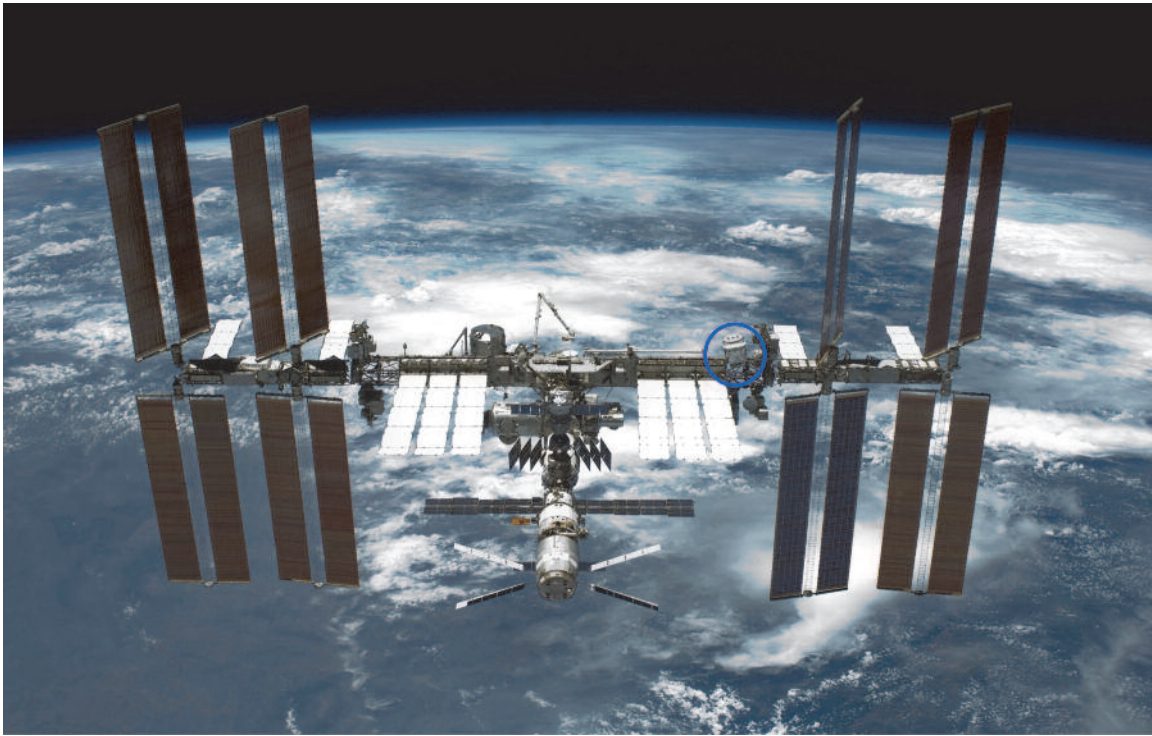


Figure 1: *The AMS Detector was installed on the International Space Station (ISS) on May 19, 2011 to conduct a program of fundamental physics research. AMS will continue to collect data for the entire lifetime of the ISS.*

The Alpha Magnetic Spectrometer (AMS) is a particle physics detector designed and built to explore some of the most fundamental issues shared by physics, astrophysics and cosmology on the origin and structure of the universe. As an external payload onboard the International Space Station, AMS will study with unprecedented precision, to one part in ten billion, the composition of primary cosmic rays originating in stars and galaxies billions of light years beyond our Milky Way. AMS originated from discussions at the Erice Center. The scientific objectives discussed in Erice included searching for cosmic antimatter, studying the origin of dark matter, and exploring cosmic rays to the TEV region. The most exciting objective of AMS is to explore the unknown from the unique vantage point of space. AMS is the first precision magnetic particle physics detector in space. AMS involves an international collaborating composed of 16

countries, sponsored by the U.S. Department of Energy (DOE) and in close cooperation with the National Aeronautics and Space Administration (NASA).

The scientific importance of AMS is based on the early seminal work of A. Zichichi as exemplified in Figures 2a, 2b, 3, 4, 5 and 6.

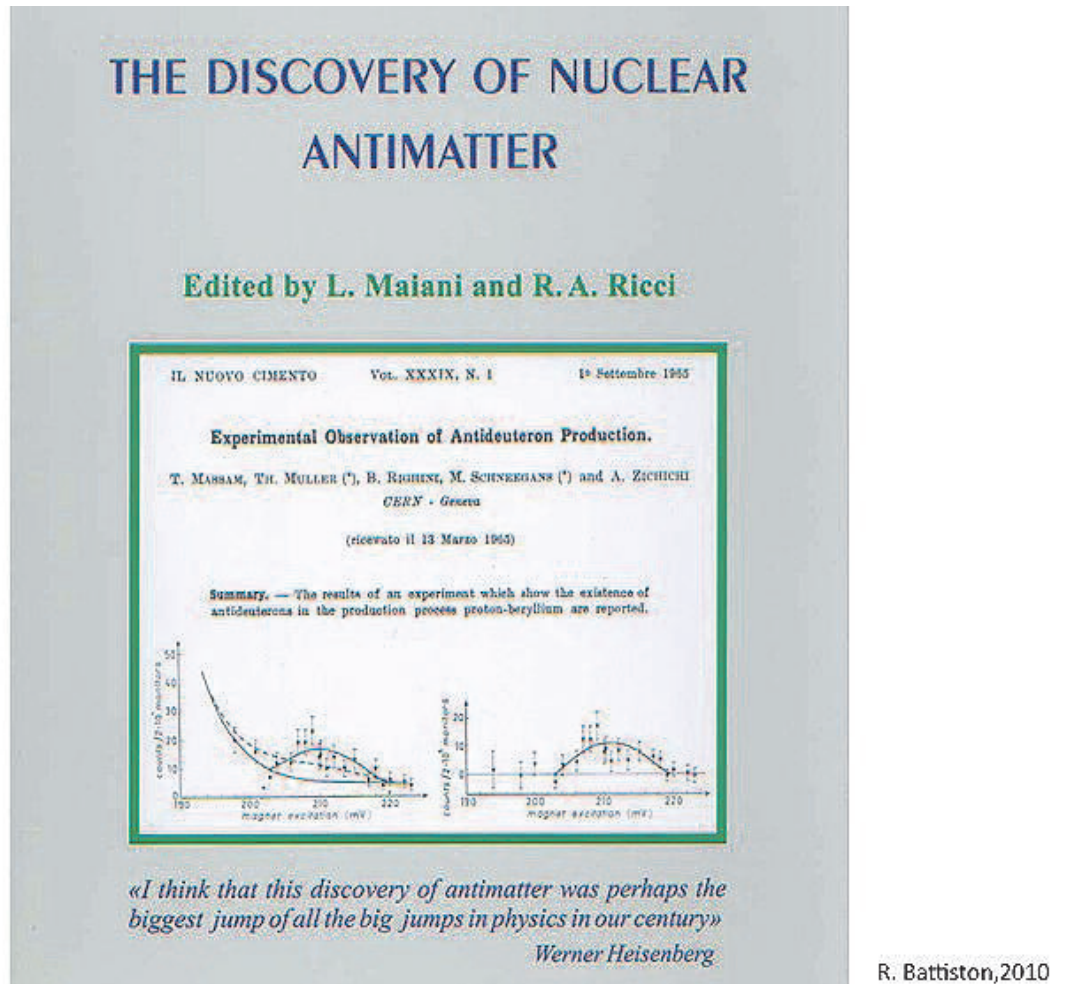


Figure 2a: *The Discovery of Nuclear Antimatter* based on seminal work by A. Zichichi on the *Experimental Observation of Antideuteron Production* (1965) published in *Il Nuovo Cimento*.

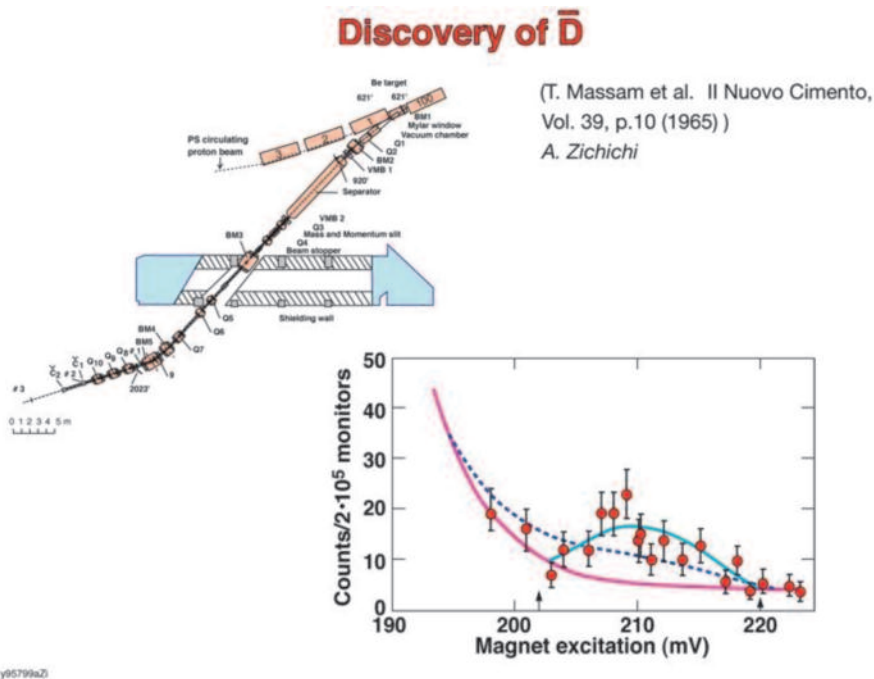


Figure 2b: *Experimental set up used in the experimental observation of Antideuteron (1965).*

Proton-Antiproton Annihilation into Electrons, Muons and Vector Bosons.

A. ZICHICHI and S. M. BERMAN (*)
 GERN - Genova

N. CAMIBBO and R. GATTO
 Università degli Studi - Roma e Cagliari
 Laboratori Nazionali di Frascati del CNEN - Roma

(ricevuto il 26 Gennaio 1962)

A. ZICHICHI · S. M. BERMAN
 1° Aprile 1962
 Il Nuovo Cimento
 Serie X, Vol. 24, pag. 170-180

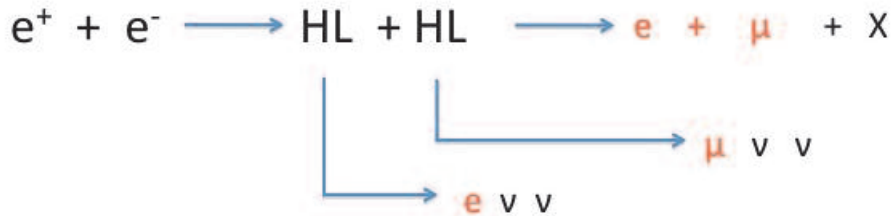
Summary. — The possibility of achieving relatively high intensity anti-proton beams has prompted some considerations on the rather rare annihilation channels of the proton-antiproton system. We propose i) to study the two-electron mode as a means of investigating the electromagnetic structure of the proton for time like momentum transfers; ii) to study the two-muon mode and compare with the two-electron mode to investigate whether the muon behaves like a heavy electron for large time like momentum transfers; iii) to investigate the existence of weak vector bosons by the modes $p + \bar{p} \rightarrow B + \bar{B}$ and $p + \bar{p} \rightarrow B + \pi$. Although no precise theoretical predictions can be made, crude estimates indicate that the cross-section for these four channels could be roughly of the same order of magnitude.

1. - The electromagnetic annihilation $p + \bar{p} \rightarrow e^+ + e^-$, $p + \bar{p} \rightarrow \mu^- + \mu^+$.

R. Battiston, 2010

Figure 3: *Summary of published results by A. Zichichi on Proton-Antiproton Annihilation into Electrons, Muons and Vector Bosons (1962).*

Search for Heavy Leptons (HL) 1970-1972(ZICHICHI)



R. Battiston,2010

Figure 4: Pioneering work by A. Zichichi on search for heavy leptons (1970-72).

Heavy Lepton search regions using the ADONE e+e- storage ring at Frascati

Limits on the Mass of Heavy Leptons, M. Bernardini, A. Zichichi et al., Nuovo Cimento 17A, 383 (1973)

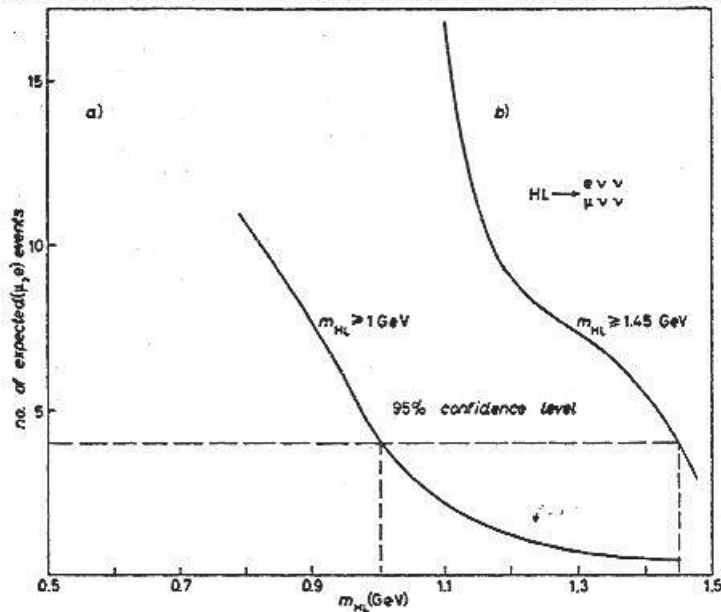


Fig. 2. - The expected number of (μ^+e^+) pairs vs. m_{HL} for two types of universal weak couplings of the heavy leptons. The dashed lines indicate the 95% confidence levels for m_{HL} . a) HL universally coupled with ordinary leptons and hadrons, b) HL universally coupled with ordinary leptons.

R. Battiston,2010

Figure 5: Published results of heavy lepton search at ADONE by A. Zichichi.

How does the muon differ from the electron?

Experiments at SLAC on muon-proton deep inelastic scattering are part of the continuing search for differences between the muon and the electron.

Martin L. Perl

34 PHYSICS TODAY / JULY 1971

Fortunately these problems can be overcome in the newly developed electron-positron colliding-beam accelerators where charged leptons can be copiously produced through the process⁵



Within five years, through this process, we shall know if the electron-muon family has additional members with masses in the several-GeV ranges.

5. V. Alles-Borelli, A. Zichichi et al., *Limits on the Electromagnetic Production of Heavy Leptons*, *Nuovo Cimento Letters* 4, 1156 (1970)

R. Battiston, 2010

Figure 6: Excerpt from *Physics Today* article dated July 1971.

Indeed, the study of leptons from pp collisions have resulted in the discoveries of the J particle, the Upsilon, the Z and W particles, and so forth.

The AMS Detector instrumentation is based on ground based accelerator physics technology but adapted to withstand the hostile environment of space, including forces of 3-12 g's at launch. For AMS, the instrumentation is required to operate flawlessly in zero gravity without the possibility of astronaut intervention for repair or maintenance.

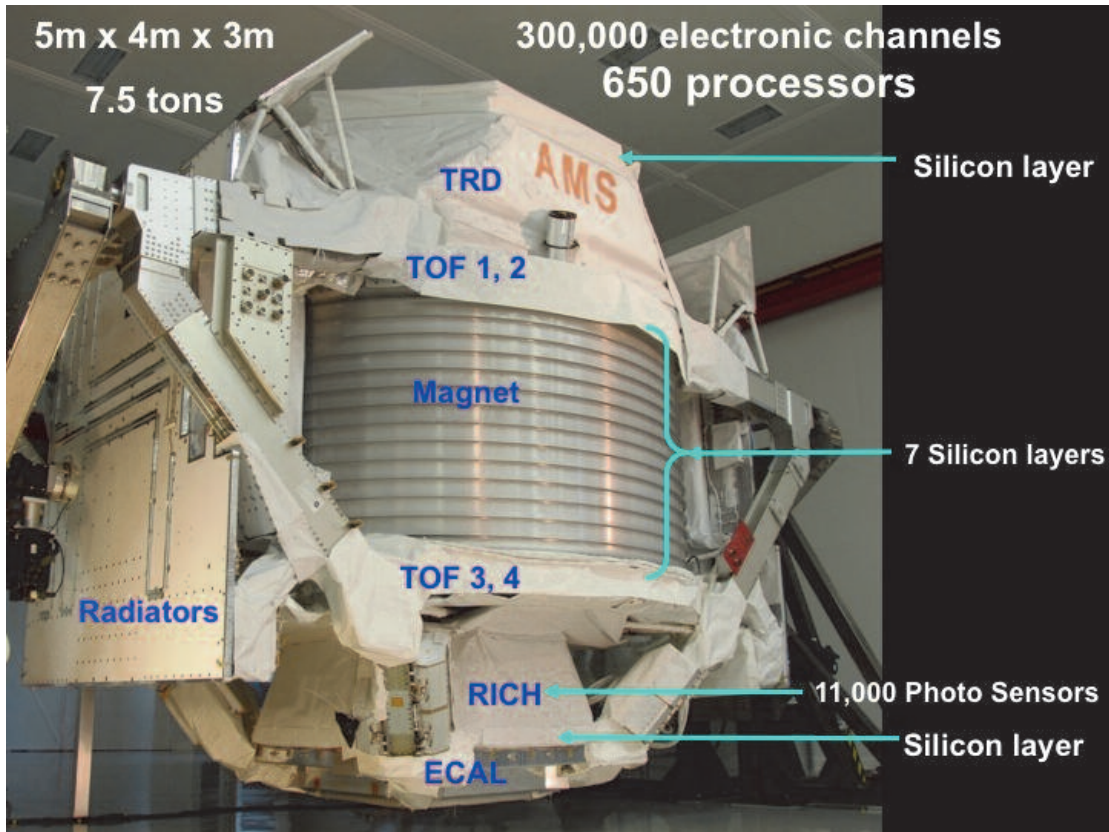


Figure 7: The 7.5 ton AMS Detector contains an array of sub-detectors, 650 processors and many complex systems to ensure its safe and successful performance in space.

As shown in Figure 7, AMS measures 5m x 4m x 3m and weighs 7.5 tons. It was built to fit within the Unique Support Structure (USS), constructed by NASA, which cradles the Detector within the shuttle cargo bay during its journey to the Space Station as well as to the attachment site on the Space Station external truss.

To ensure mission success, many modules were constructed for each sub-detector component, the magnet and the 60 microprocessors (Engineering modules (EM), qualification modules (QM), flight modules (FM) and flight spare modules (FS)), so that every system could be thoroughly tested and space qualified. Multiple redundancies have been built in every flight system, some as much as 400%. Associated with the detector instrumentation, are complex systems such as ultra fast electronics, thermal control, ground and flight software, alignment and positioning systems, interface and support structures, etc. These systems have also been developed specifically for AMS and have pushed existing technology to the limit.

Since particles are defined by their mass, charge and energy, the AMS Detector has been designed and built to contain a magnet and an array of the state of the art precision particle detectors. Together, this instrumentation defines and characterizes the charged particles that pass through AMS from the far reaches of space. The main subdetector components and their functions are illustrated in Figure 8.

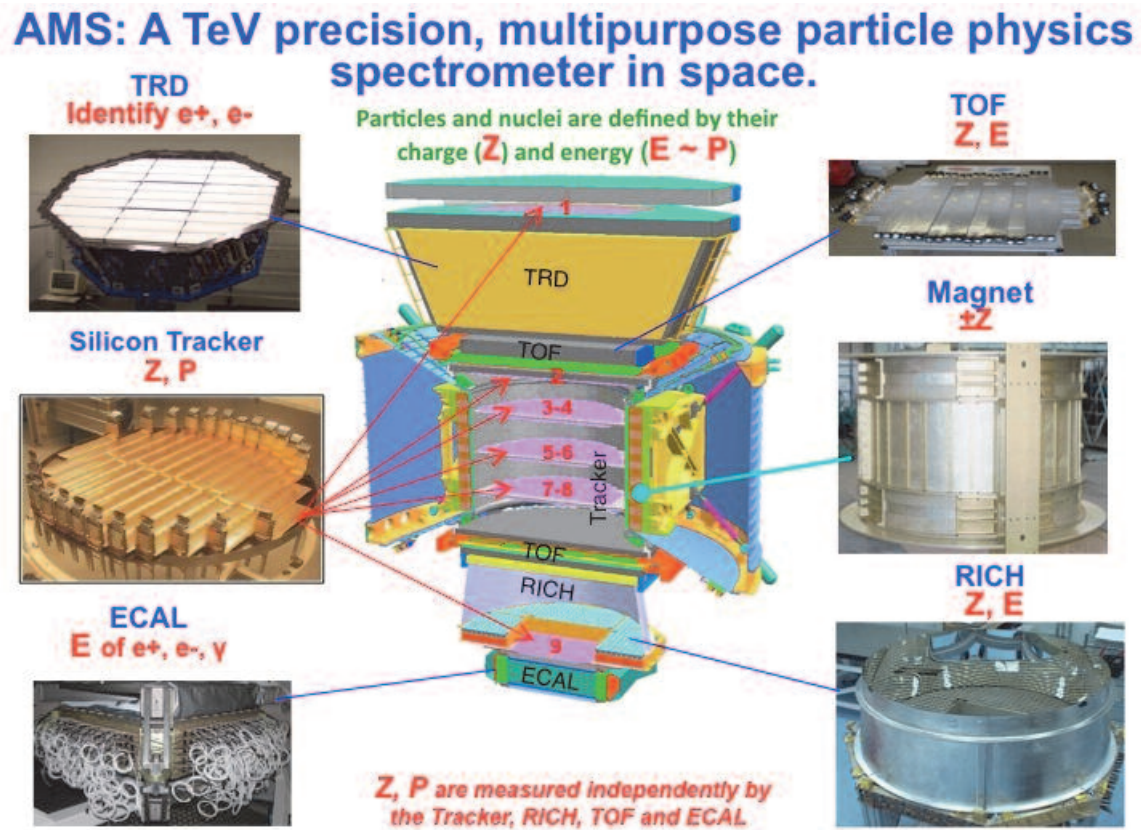


Figure 8: Cut-away view of the AMS Detector showing the arrangement of its precision detector components.

The centerpiece of the AMS Detector is the large volume permanent magnet that measures the sign of the charge and momentum of each particle traversing AMS. Particles and anti-particles will be identified according to their bending trajectories in the magnetic field.

The magnet was made of 4,000 blocks of Neo-dymium Iron Boron ($Nd_2Fe_{14}B$) with a field intensity of 1,400 Gauss. The magnet was flown successfully on the ten day AMS-01 mission (STS-91) in 1998. Thirteen years after this flight, the magnet was tested and the field map showed no change in the magnetic field with the experimental

accuracy of about 1%. Originally built in China, there were ten magnets fabricated for tests including one to test to destruction. The magnet was designed and built to eliminate the effect of torque on the Shuttle or ISS instruments and underwent intensive space qualification testing including vibration, centrifugal acceleration and static loading. The magnet was approved and certified for flight by the AMS NASA Lockheed Martin team.

The Magnet

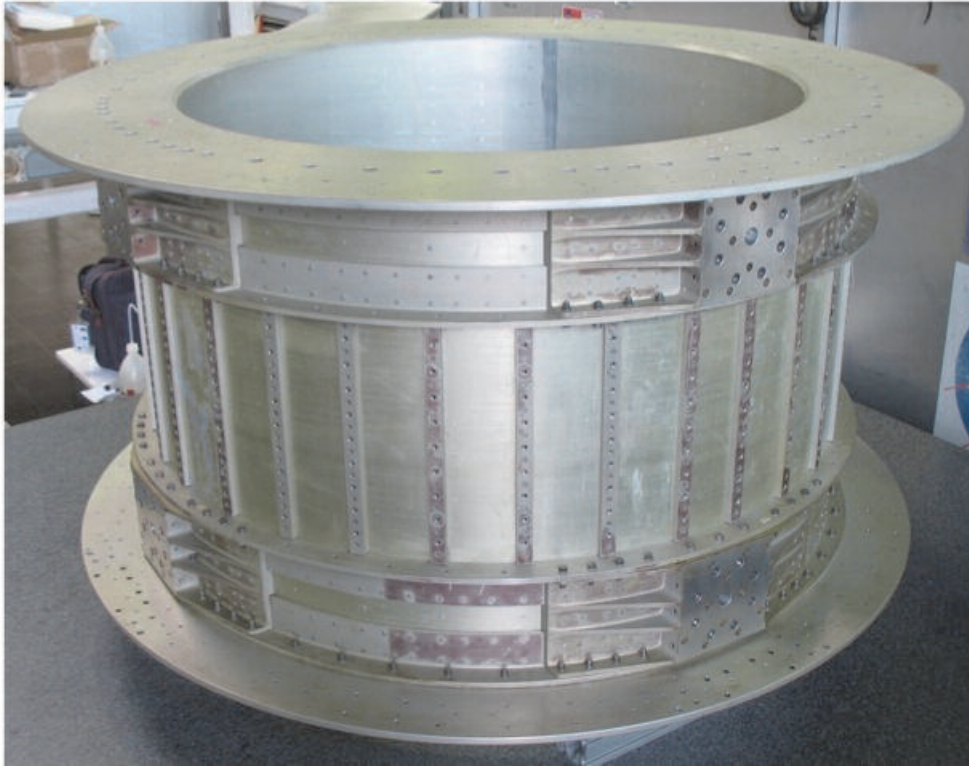


Figure 9: *The AMS Permanent Magnet was flown in the AMS-01 mission (STS-91) in 1998 and in the AMS-02 mission on the ISS in 2011.*

The extended lifetime of the International Space Station agreed by NASA and all the ISS international partners meant that the AMS Experiment would be active for more than the three years as originally planned with the use of a superconducting magnet. To remain operational for the full lifetime of the ISS, the AMS Collaboration installed the Permanent Magnet and optimized the geometry of the Detector by adding more silicon planes and rearranging the existing silicon planes thereby increasing the measurement arm. This technique recovered the full sensitivity (within 10% or less) for AMS on matter antimatter separation and tests showed that the momentum resolution is maintained.

As seen in Figure 8, the Transition Radiation Detector (TRD) is located on the upper portion of the AMS Detector. Its purpose is to identify and distinguish electrons and positrons from other cosmic rays. Since positrons can be mistaken for protons at high energies, the TRD suppresses the proton background which is important in the search for Dark Matter. Unlike the proton, the electrons and positrons emit transition radiation gamma rays while crossing the TRD radiator surfaces. These gamma rays are recorded when electrons and positrons pass through the 20 layers of 6mm diameter straw tubes alternating with 20 layers of polyethylene/polypropylene fleece radiator. The large number of surfaces increases the probability of the production of transition radiation gamma rays. As electrons and positrons pass through the TRD, the gamma rays start an ionizing cascade near a gold plated thin wire at high voltage. The abrupt current change induces a fast electric signal that can be read out at the end of the wire through a custom made Data Acquisition (DAQ) Microprocessor system. In this way, the identification of electrons and positrons is determined and protons are rejected. Of the 9,000 proportional mode straw tubes built, 5,248 were selected based on their leak rate. Samples were measured in a CAT scan at a hospital during night time hours to verify the centering accuracy of the signal wires to 100microns. The leak tight straw tubes are filled with an 80/20 ratio mixture of Xenon and CO₂ at 1 bar absolute pressure from a re-circulating gas system. The gas system is carefully regulated to eliminate contamination and ensure stable pressure. Gas supply and circulation is continuously monitored. The endurance of the consumables based on usage and leak rate has been studied and data has shown that the consumables are sufficient to maintain the operation of the TRD for 20 years in space.

Transition Radiation Detector: TRD

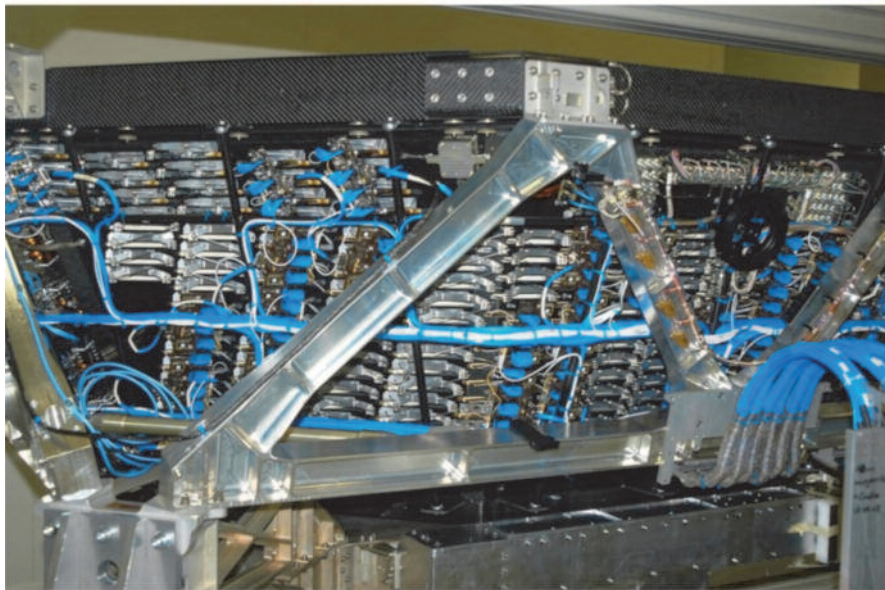


Figure 10: *The octagonal mechanical structure of the Transition Radiation Detector was made of a light-weight carbon fiber and aluminum honeycomb sandwich material to support the 328 modules. Each module contains 16 straw tubes interleaved with the 20 layers of fleece radiators.*

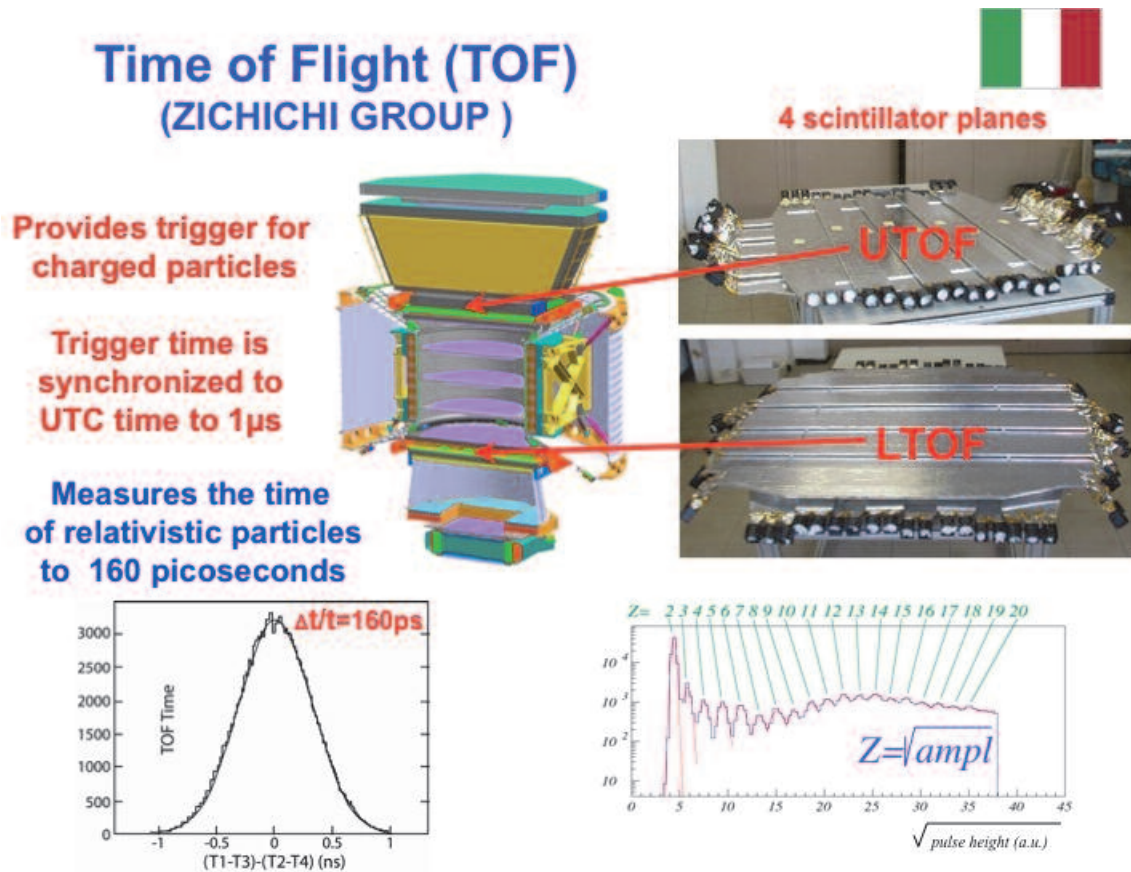


Figure 11: The Time of Flight system consists of four planes of scintillation counters containing paddles aligned along the x and y coordinates. Plexiglass light guides connect the scintillator assemblies to photomultipliers (PMTs). The light emitted by the charged particles interacting with the scintillating medium is collected by the light guides on the PMTs which convert the fluorescence light into a signal.

The upper and lower layers of the TOF detects the incoming signal of cosmic rays as well as measuring the mass, charge and energy of charged particles. The trigger time for the entrance and exit of the charged particles through the TOF is synchronized to the Universal Time Clock (UTC) to 1 microsecond. The upper and lower TOF measure the time of relativistic particles to 160 picoseconds as they travel at a velocity up to the speed of light.

When a particle enters the Upper and Lower TOF it triggers all the AMS subdetectors (Tracker, TRD and E-cal...) to collect data which is subsequently processed and stored. The level 1 trigger of the data acquisition system is initiated using information from the TOF (for charged particles), ACC (for veto information) and E-cal (for neutral particles). In addition, the TOF is capable of providing reliable information on the absolute charge of a particle that will definitively identify nuclei such as Helium, Carbon, Silicon and so forth.



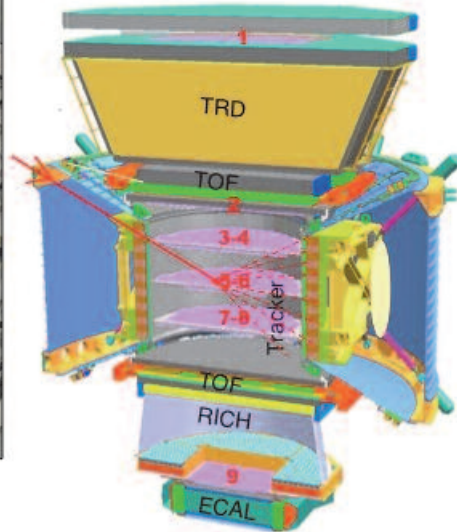
Figure 12: *Professor A. Zichichi and physicists from INFN/Bologna at the AMS Clean Room at CERN during AMS Detector assembly.*

The array of Anti-Coincidence Counters (ACC) makes up the Veto system. The counters provide a signal that a cosmic ray has entered the detector side-ways. AMS is designed to analyze only particles that traverse the whole detector from the top to the bottom so the ACC counters reject the stray cosmic rays out of the two thousand particles per second, that traverse AMS. The veto system has been designed and tested to reach an efficiency of 0.99999.

The ACC consists of 16 paddles arranged on a cylindrical barrel surrounding the Tracker. The light coming from the scintillating paddles is collected in wavelength shifting fibers of 1 mm diameter embedded in grooves milled into the scintillation material. At both ends of the paddle, fibers are routed in 2 bunches of 37 fibers each to optical connectors located on the conical flanges of the magnet vacuum case (see Figure 13). From these connectors the light goes through clear fibers to 8 photomultiplier tubes (PMT) mounted on the rim of the vacuum case. The PMTs are oriented with axes parallel to the stray field in order to minimize the magnetic field effect.



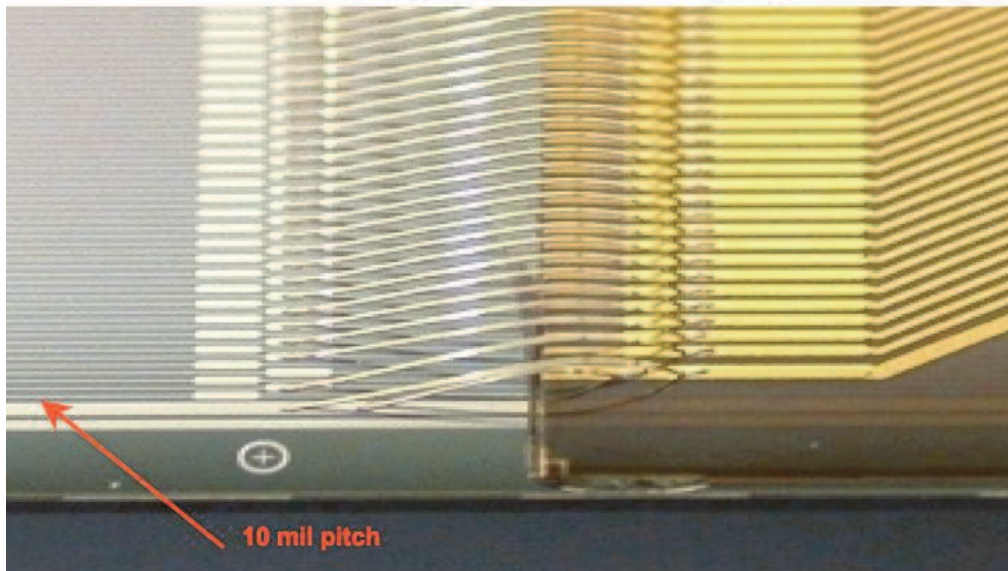
Veto System rejects random cosmic rays



Measured veto efficiency better than 0.99999

Figure 13: The installation of the Anti-Coincidence Counters (ACC) into AMS at CERN.

Silicon Tracker



The coordinate resolution is 10 micron

Figure 14: A view of the Silicon Tracker wafers and microbonds under a microscope. The Tracker provides a coordinate resolution of 10 microns.

The Silicon Tracker contains 200,000 channels. Nine layers of precision silicon measure the charge and momentum of the particles with unprecedented accuracy (a coordinate resolution of 10 microns).

The Tracker measures the curvature of the particles traversing the magnet. The curvature measurement allows the particle momentum (mass multiplied by velocity) to be determined. The pulse height in the Tracker measures the charge Z of the incoming nuclei or particle. Particle rigidity is the particle momentum divided by charge ($R=p/Z$). High energy particles are more rigid than low energy particles. Two particles with the same momentum could have different rigidities (i.e., the one with the higher charge is less rigid than the others). Since the Tracker measures the curvature, the corresponding rigidity can be immediately derived and if the charge Z is also measured then the particle momentum can be calculated.

The basic element of the Tracker is the double-sided micro strip sensor. There are 2,264 such sensors assembled in 192 readout units, called ladders. Each sensor consists of a substrate of high purity doped silicon 300 μm thick. The two sides of the substrate aluminum strips run in orthogonal directions. A position resolution of 10 μm is provided when a charged particle crosses the silicon substrate. The sum of the electric signals on the strips is proportional to the square of the absolute charge of the particle. The online processing of the Tracker data is performed by the dedicated Tracker Data Reduction boards. The readout electronics are characterized by a very low power consumption with low noise and large dynamic range.

There are 9 planes with 200,000 channels aligned to 3 microns



Figure 15: There are a total of nine Tracker planes. Seven Tracker planes are located within the magnet bore, one is mounted on top of the TRD and one is mounted below the RICH detector.

The Ring Image Cerenkov Counter (RICH) measures the charge and energy of passing particles by precisely determining their velocities with an accuracy of 0.1%. Both the charge and the velocity are calculated from the geometrical shapes, circles or rings, generated by the Cerenkov effect.

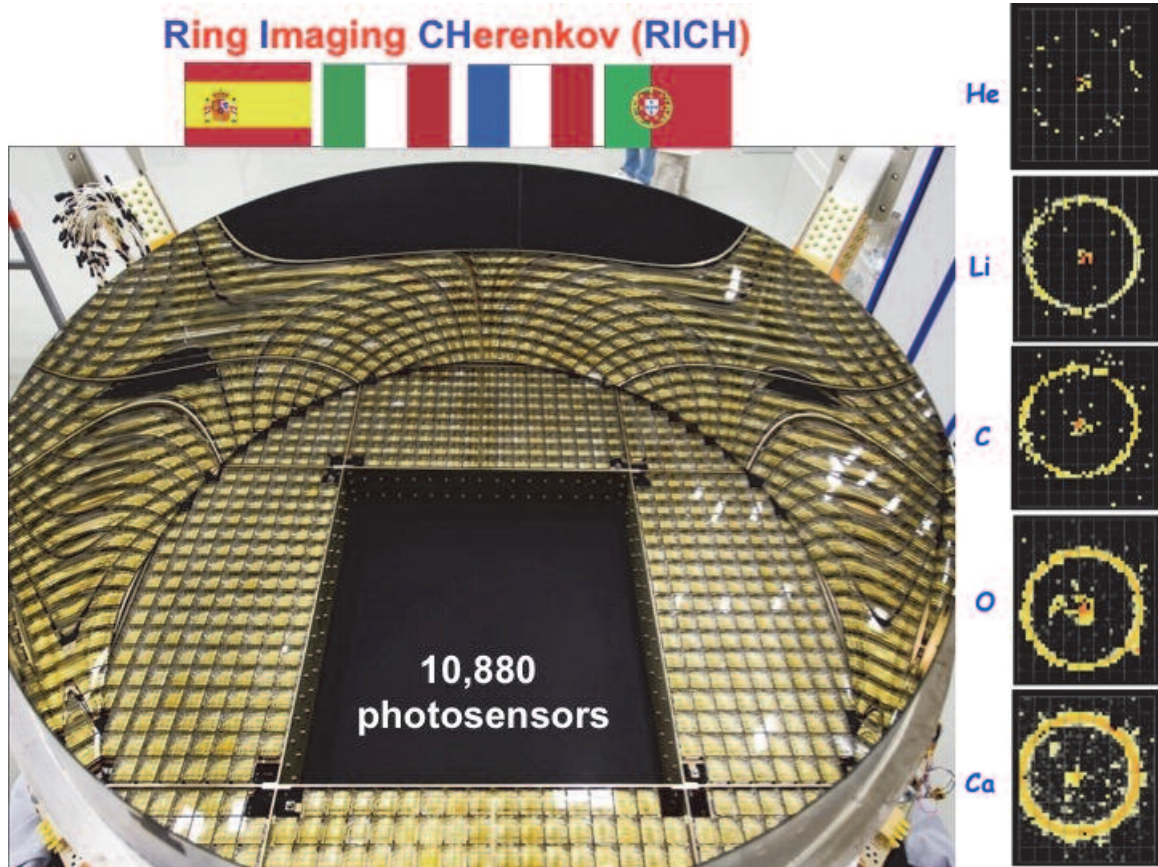


Figure 16: The RICH contains 10,880 photosensors to measure the velocity and charge of passing particles.

The RICH detector consists of a radiator plane, a conical mirror and a photon detection plane. The radiator produces the Cerenkov radiation with an array of 2,7 cm thick aerogel tiles and a refractive index between 1.03 surrounding a central region equipped with 5mm thick Sodium Fluoride (NaF) with a refractive index of 1.3. This combination optimizes the overall acceptance for different energy ranges since the Cerenkov photons radiated by the NaF in a large cone will fall within the detection area. The detector plane has an empty area in its center that matches the active area of the Ecal that is located immediately below the RICH. Around the exterior of the open space, 10,880 photosensors are arranged in a matrix to cover the circular surface at the bottom of the conical mirror. The radiator and the detection plane are enclosed in the column of the conical reflector multi-layer structure on a carbon fiber reinforced composite substrate.

The mirror amplifies the RICH acceptance reflecting high inclination photons and provides the necessary photon drift ring expansion.

Mass and nuclear charge are fundamental properties of particles and nuclei. Mass and charge are independently measured in AMS through the Tracker, Time of Flight and RICH. Velocity is measured by the RICH and Time of Flight. The RICH was designed to provide velocity measurements with a resolution of 0.1% for charged particles and $\sim 0.01\%$ for ions. Since energy is dependent on velocity $= \frac{1}{2}mv^2$, the RICH with its accurate velocity can be measured to an accuracy of 1/1000 and simultaneously nuclear charge can be identified up to Cu.

The Electromagnetic Calorimeter (E-cal) is a 3-dimensional instrument made of 1,200 lbs of lead sandwich and 50,000 optical fibers and measures the energy and direction of TeV light rays and electrons with high precision (see Figures 17 and 18).

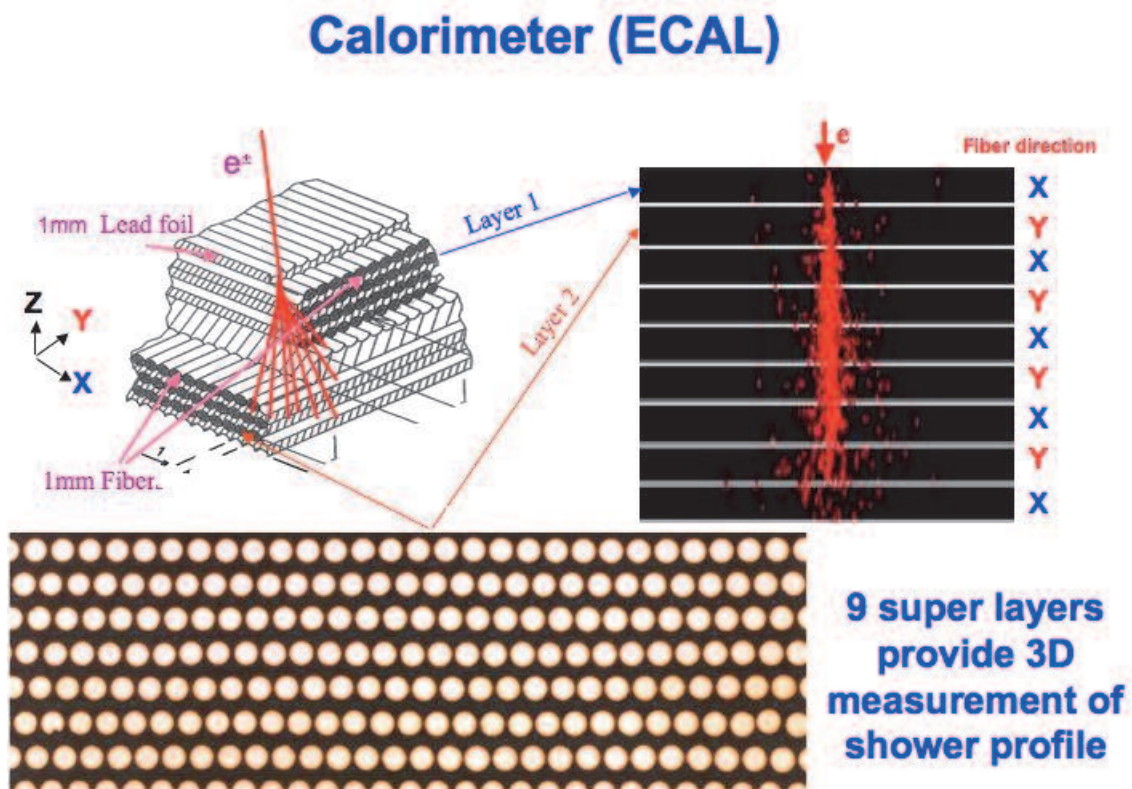
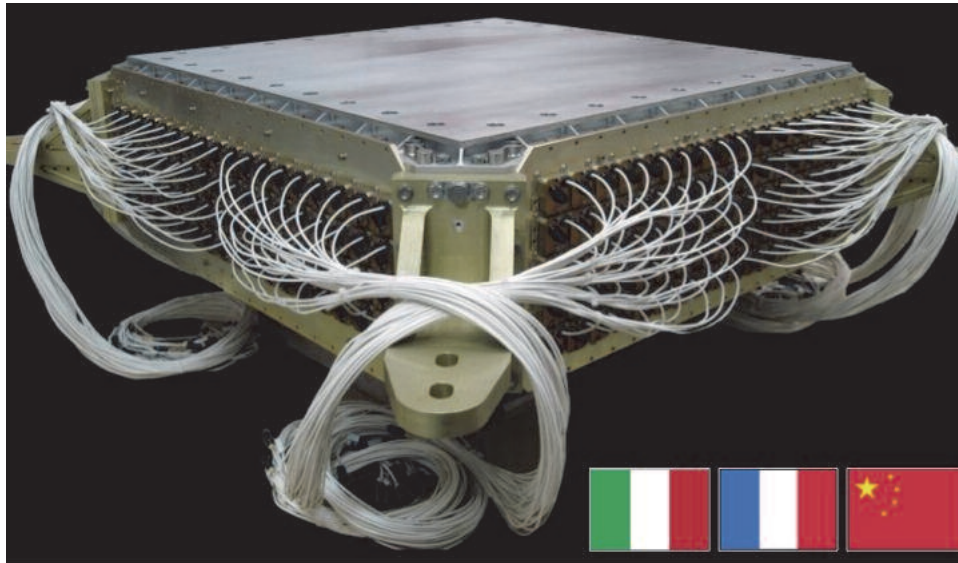


Figure 17: The principle and structure of the Electromagnetic Calorimeter.

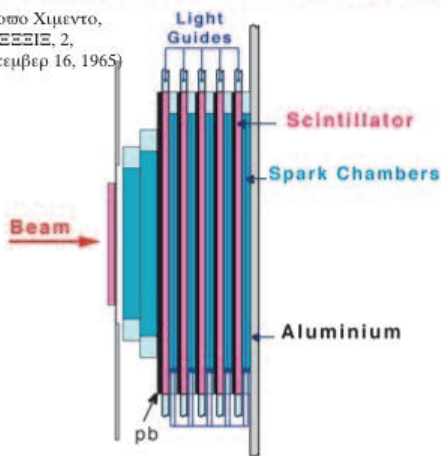


50,000 fibers, $\phi = 1\text{mm}$, distributed uniformly inside 1,200 lb of lead which provides a precision, 3-dimensional, $17X_0$ measurement of the directions and energies of light rays and electrons up to 1 TeV

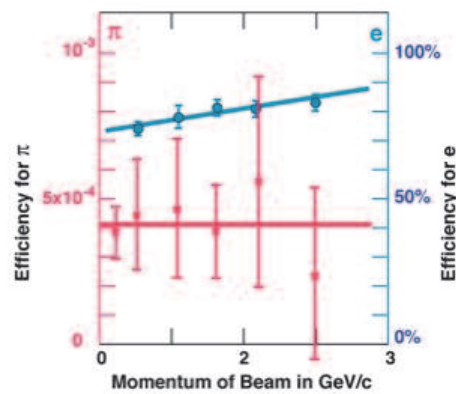
Figure 18: *Two Electromagnetic Calorimeters were built: one for space qualification tests and one for flight.*

Zichichi and his collaborators have continued the development of instrumentation to find a way to improve the e/π rejection to order of 10^{-4}

(Νυστω Χιμεντο, ζολ. ΞΞΞΙΞ, 2, Σεπτεμβρι 16, 1965)



Electron detector, which consists of five elements, each one being made of a lead layer followed by a plastic scintillation counter and a two-gap spark chamber.



The rejection power of this new detector against pions is of the order of a $4 \cdot 10^{-4}$. The efficiency for electron detection varies from 75% to 85% (right scale) and the energy resolution can be as good as 10%, in the energy range 1.1 GeV to 2.5 GeV.

y94294_03

Figure 19: *Successful instrumentation development using an electron detector has been carried out by A. Zichichi and his collaborators to significantly improve the rejection power against pions.*

The E-cal consists of a pancake structure composed of 9 superlayers. Each superlayer is 18.5mm thick and is made of 11 grooved, 1 mm thick lead foils interleaved with layers of 1mm diameter scintillating fibers glued together. The detector imaging capability is obtained by arranging the superlayers with fibers alternating parallel to the x axis (5 layers) and y Axis (4 layers). Electrons, positrons and gamma rays interact in the dense material of the E-cal producing an electromagnetic shower of lower energy particles. From the shape of the shower it is possible to reconstruct the direction and energy of the incident particle. This is particularly important for the measurements of high energy photons. The shower ends either when secondary particles are absorbed or when they are able to escape from the material. In this way the E-cal distinguishes positrons and protons. Protons and heavy nuclei interact in a different way producing a different type of shower with a characteristic wider shape. The shower shape can also contribute to the reconstruction of the direction of the incident particle to a precision of a few degrees. Also, the E-cal is able to follow a 3-D shower profile at 18 different depths. Its precision will enable AMS to identify one positron from 10,000 protons. The E-cal thus works in concert with the TRD in its powerful rejection capability of protons and nuclei. The AMS E-cal follows the original development on preshower sampling technology invented by A. Zichichi as shown in Figure 19.

The ultra-precision of the AMS detector enables it to measure the particles with an accuracy of:

1) the coordinates to 10 microns; 2) the travel time to 160 ps; and 3) the velocity to an accuracy of 1 in 1000.

It will also simultaneously measure all cosmic ray atomic nuclei to an energy of a trillion electron volts (see Figure 20).

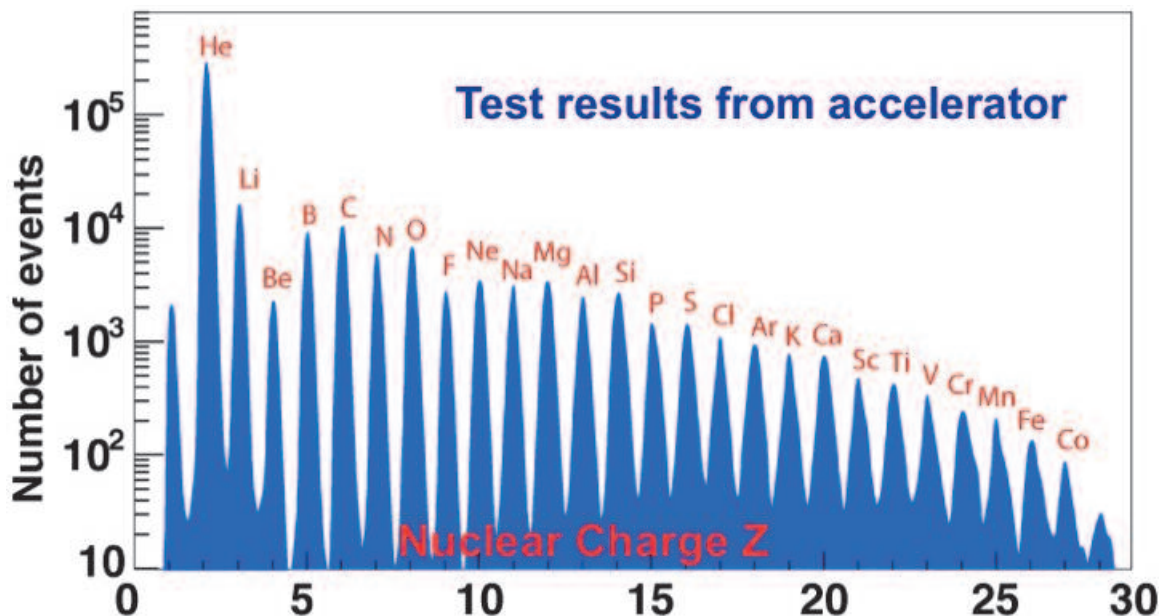


Figure 20: *With its ultraprecise detectors and resolution, AMS will measure cosmic ray spectra for nuclei, for energies from 100 MeV to 2 TeV, with 1% accuracy over the 11 year solar cycle.*

Figure 21 illustrates the scope of the AMS Collaboration.

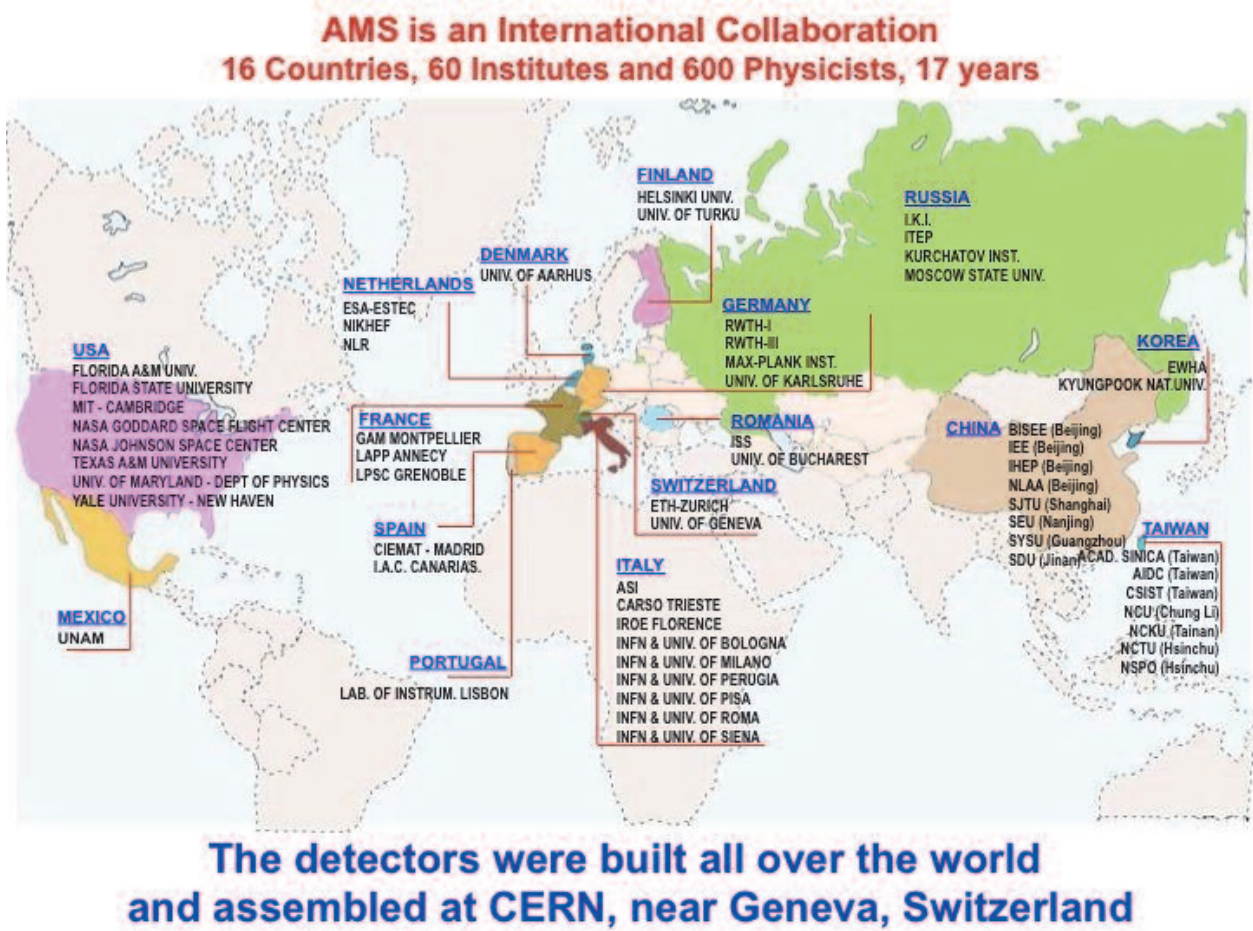


Figure 21: *The scope of the AMS international collaboration.*

After completion of detector assembly at CERN, AMS was moved to the European Space Agency Technology Center (ESTEC) in Noordwijk, the Netherlands for Thermal Vacuum Test and EMI/EMC tests in their unique facilities. The Large Space Simulator (LSS) at ESTEC is shown in Figure 22. The LSS measures 15 meters in height and 10 meters in diameter. Its powerful xenon lamps simulate the temperature of the sun and liquid nitrogen cooled walls simulate the opposite extreme of temperature in space.

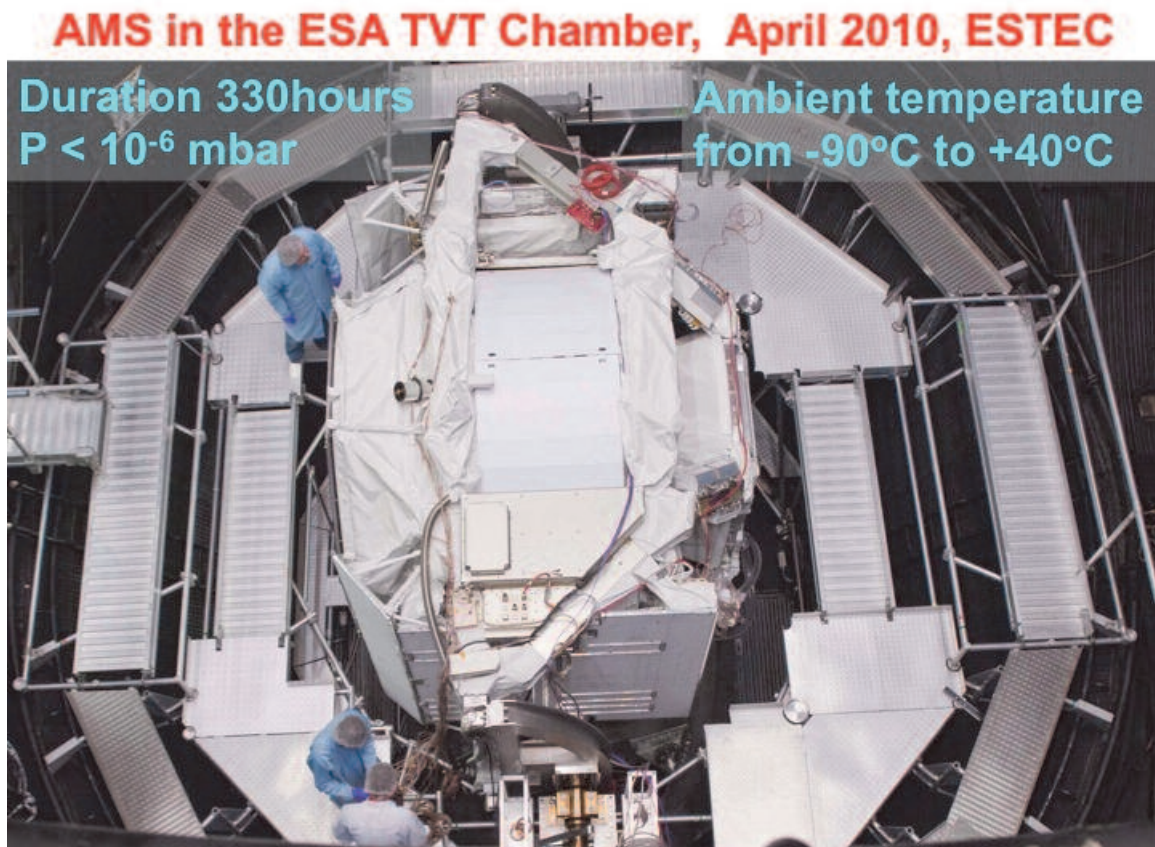


Figure 22: *The completed AMS Detector underwent crucial thermal vacuum testing and EMC testing at the European Space Agency Technology Center (ESTEC) in Noordwijk, the Netherlands to test the performance of the Detector in space flight conditions.*

In addition to Thermal Vacuum Testing, AMS underwent EMI and EMC testing in ESTEC's Maxwell Test Chamber. Results verified that AMS systems and the ISS and Shuttle systems do not generate any electromagnetic interference that might have an adverse affect on each other's performances.

Following the test procedures at ESTEC, AMS was moved back to CERN-Geneva to undergo test beam calibration. Figure 23 shows the AMS Detector in the CERN test beam and the results are shown in Figures 24 and 25.

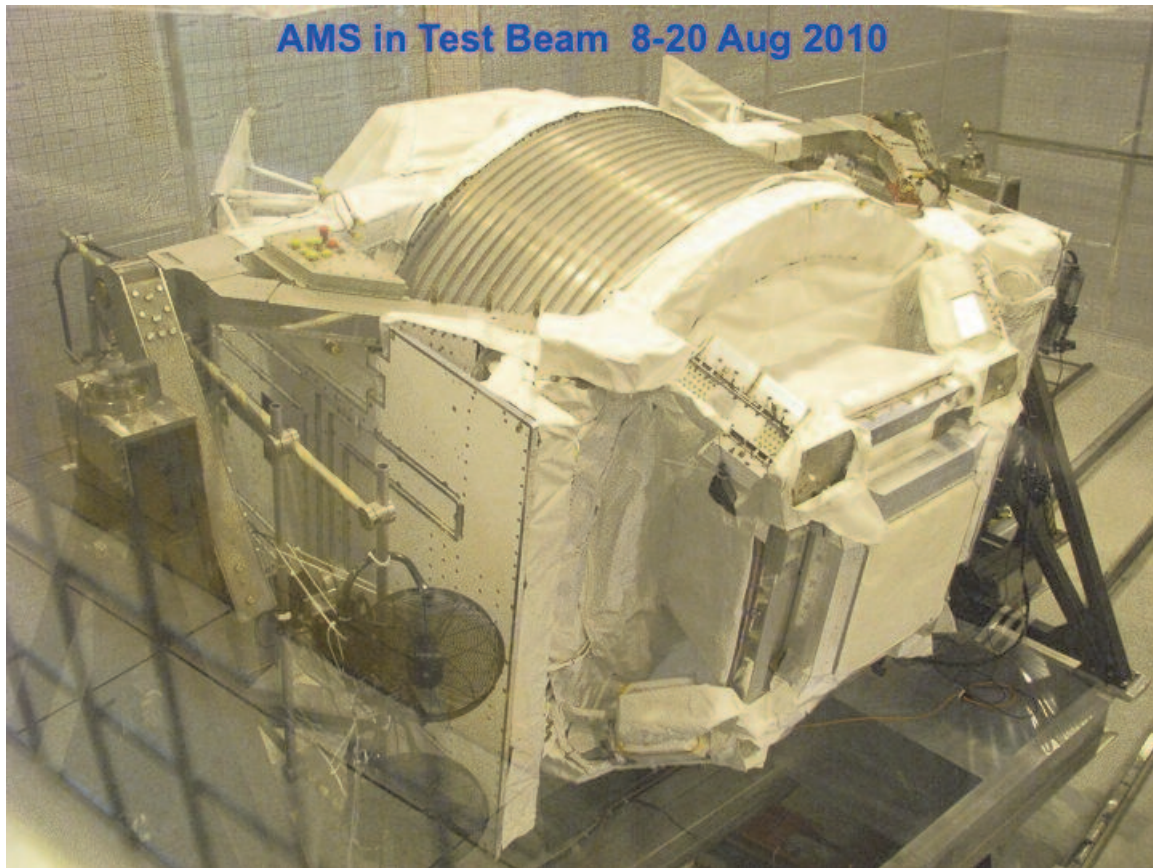


Figure 23: *CERN provided test beam time from its accelerator complex to calibrate AMS.*

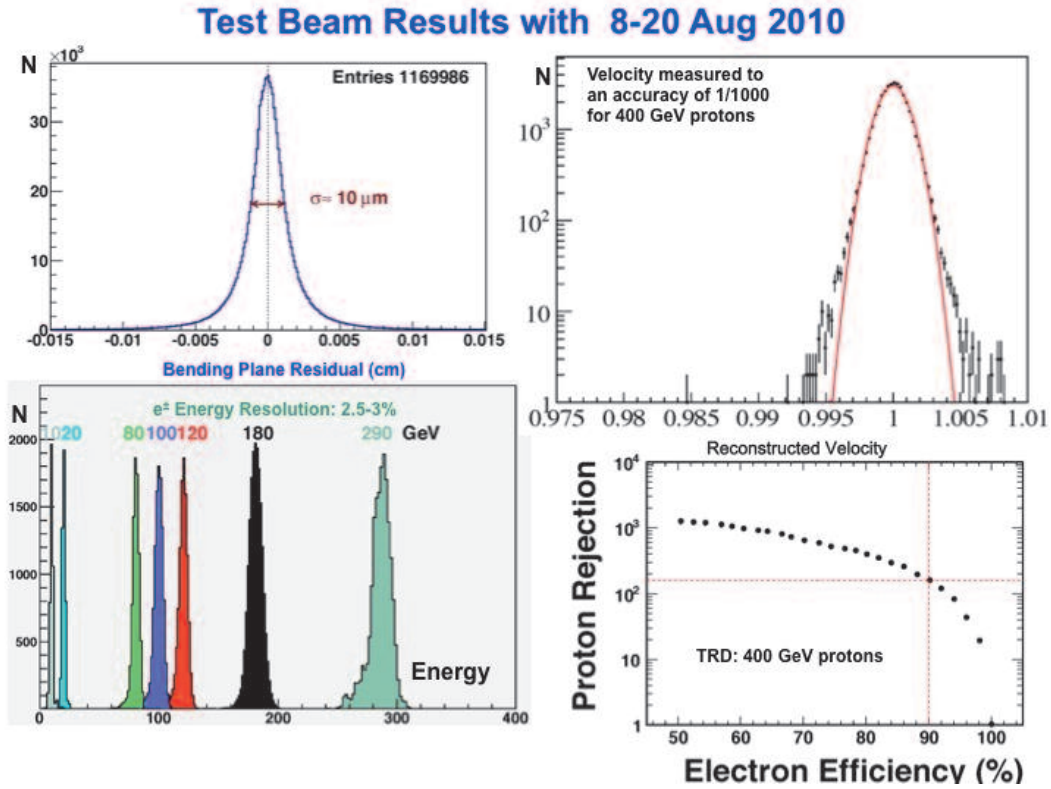


Figure 24: AMS test beam results from CERN accelerator beam (2010) prior to AMS departed to Kennedy Space Center.

Rigidity resolution

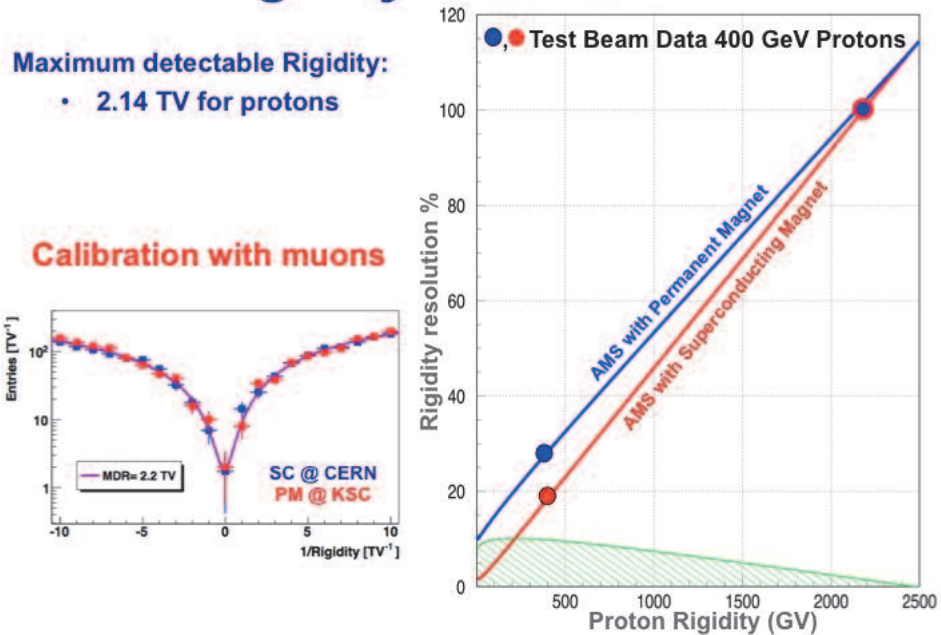


Figure 25: AMS test beam data showing measurements of 400 GeV proton rigidity resolution for the superconducting magnet and the permanent magnet.

AMS was delivered to the Kennedy Space Center from Geneva on August 26, 2010 in a special U.S. Air Force C5-M aircraft. Landing on the Shuttle Landing facility at Kennedy Space Center, AMS was immediately transported to the Space Station Processing Facility (SSPF) at KSC for preflight testing and processing.

Figure 26 through Figure 38 illustrate activities at Kennedy Space Center including the launch of STS-134, docking with the ISS and deployment of AMS on the ISS on 19 May 2011.

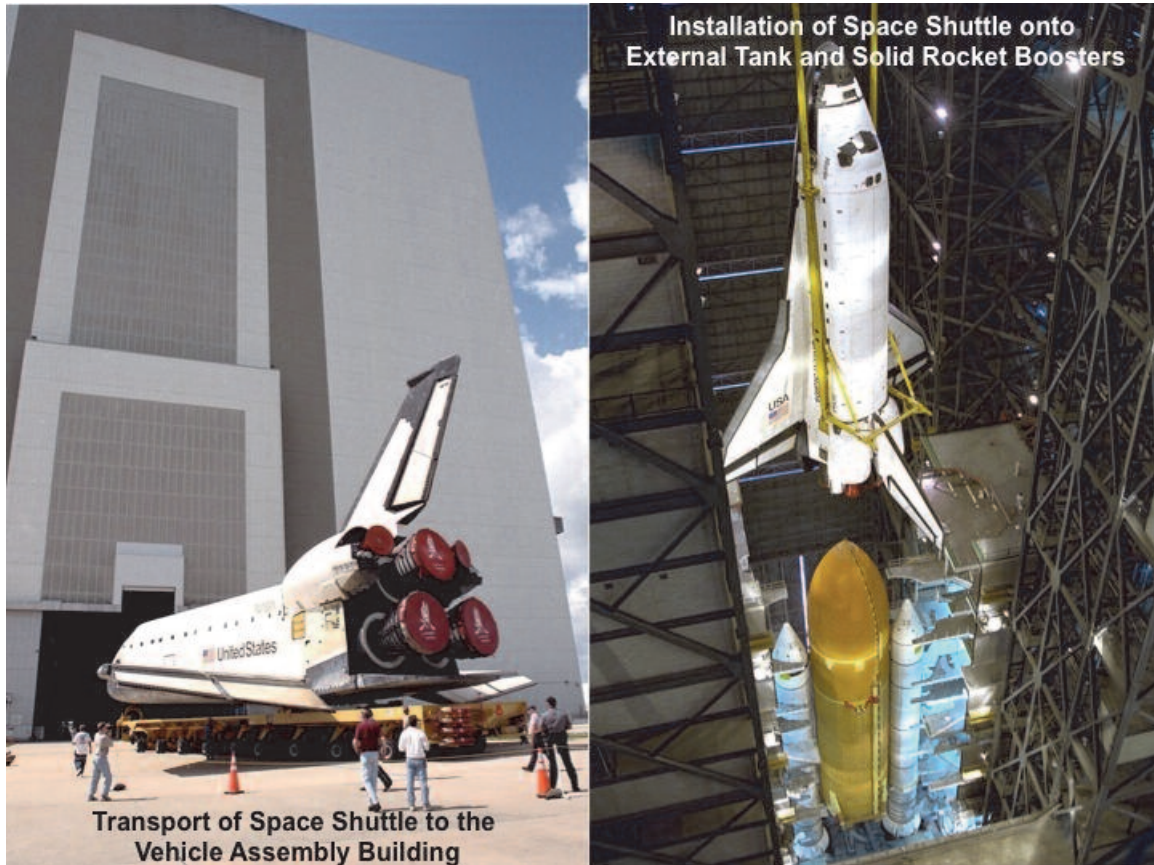
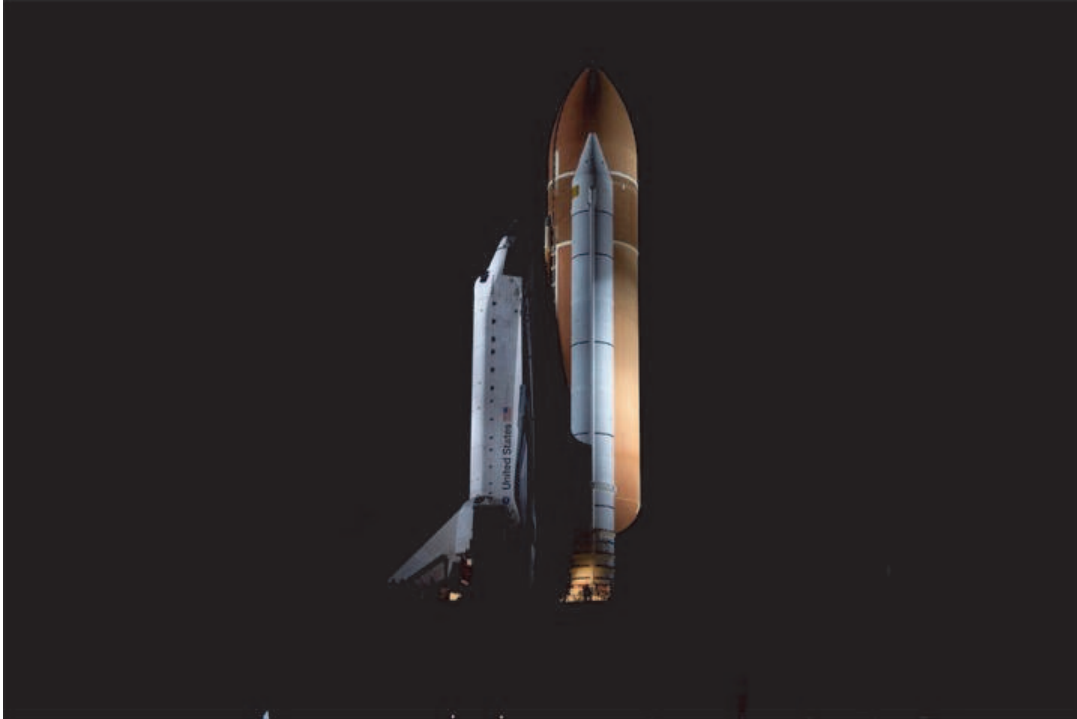
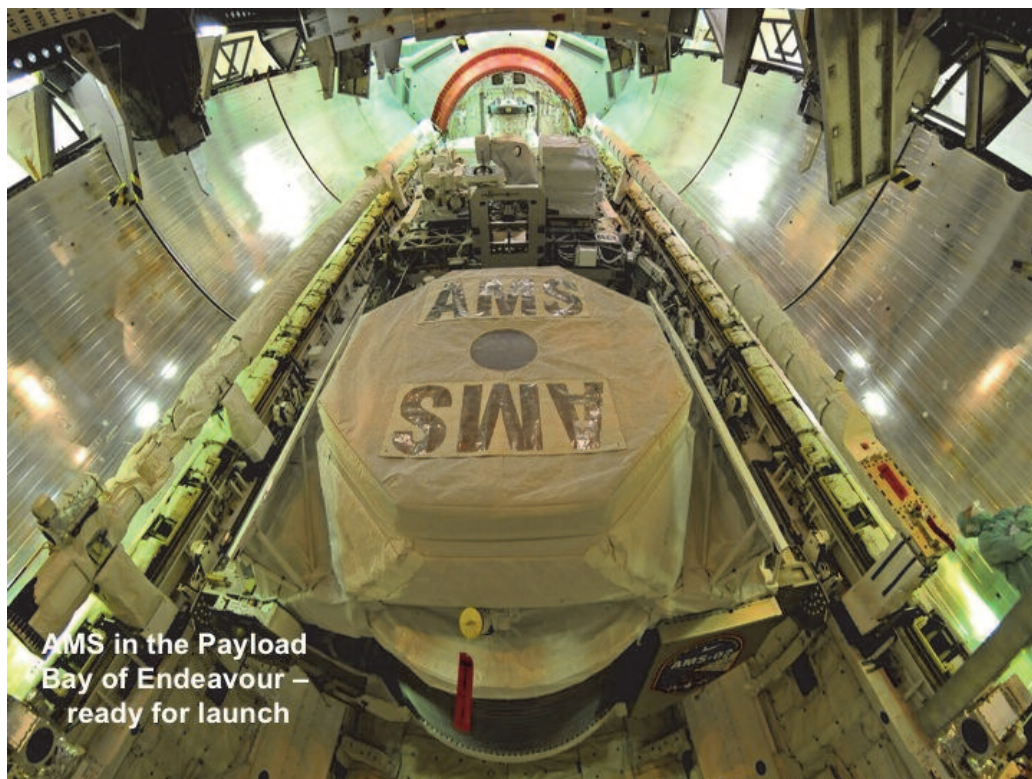


Figure 26: Orbiter *Endeavour* being prepared at Kennedy Space Center for its final launch to carry AMS to the ISS. Left: *Endeavour* entering the Vehicle Assembly Building (VAB). Right: *Endeavour* being mated with its large External Tank and two Solid Rocket Boosters (SRB) in the VAB.



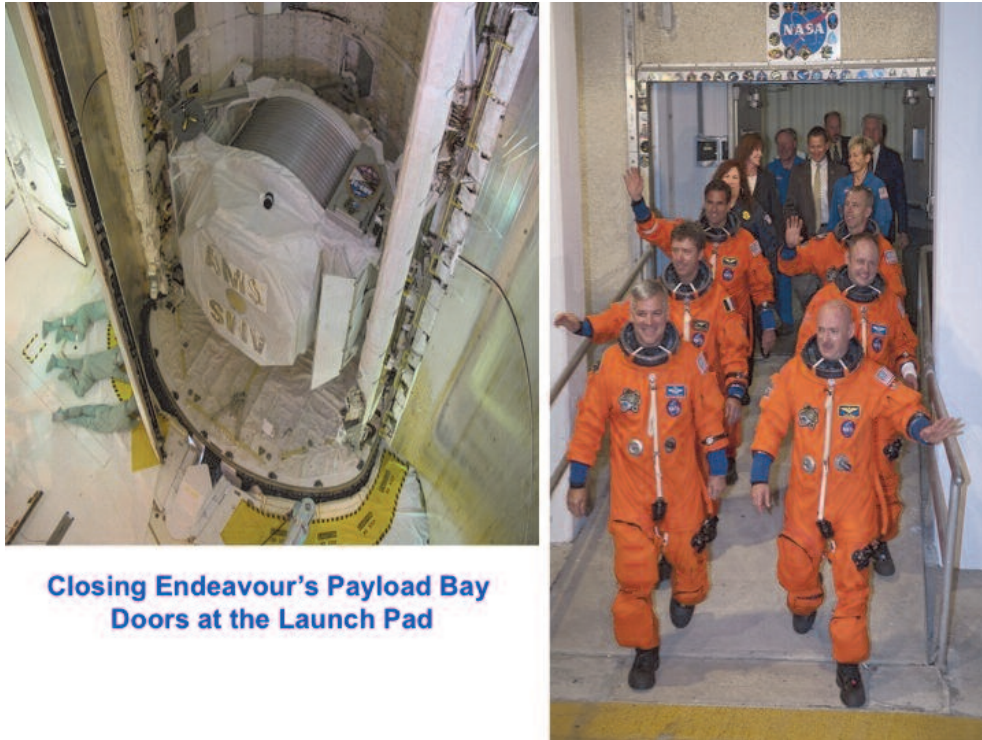
Transfer of STS-134 to the launch pad

Figure 27: Orbiter *Endeavour* being rolled out to Launch Pad 39A at Kennedy Space Center (March 2011) to await launch.



AMS in the Payload Bay of Endeavour – ready for launch

Figure 28: A view of AMS installed in *Endeavour's* cargo bay awaiting launch.



Closing Endeavour's Payload Bay Doors at the Launch Pad

Figure 29: *Left: Closing of Endeavour's payload bay doors prior to launch. Right: The crew of STS-134, under the command of Captain Mark Kelly (USN), proceed to the launch pad on May 16, 2011. Among the six member crew was Colonel Roberto Vittori, ESA and Italian Air Force, who is seen in the second row, left side.*

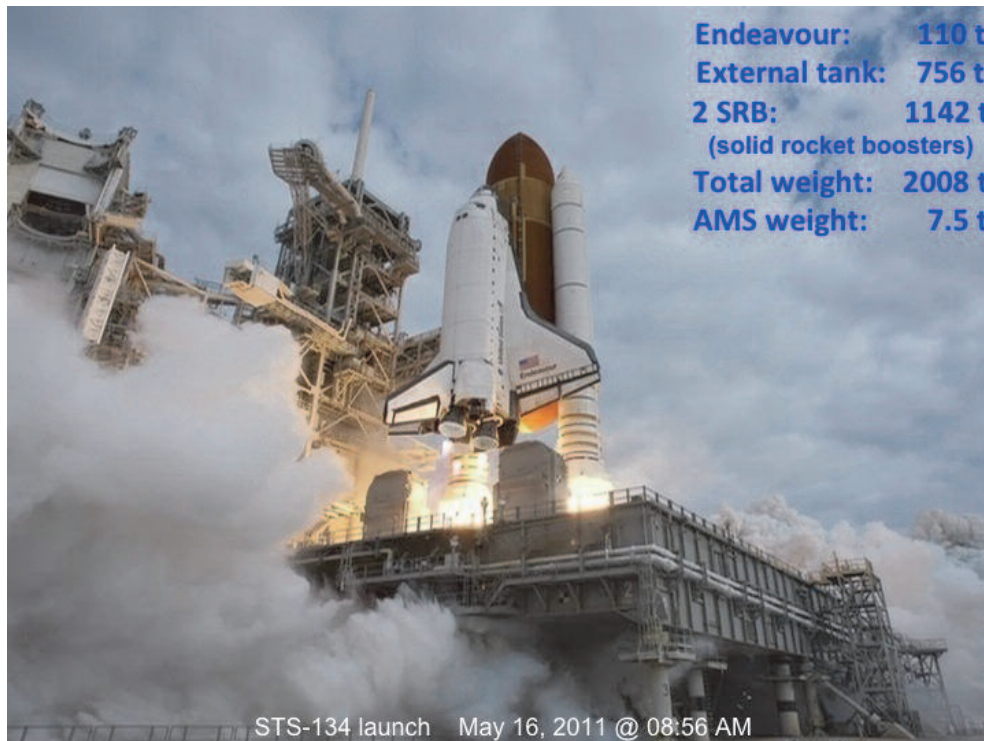


Figure 30: *The final launch of Endeavour carrying AMS to the International Space Station took place on May 16, 2011 at 0856.*



Figure 31: Seconds after launch, *Endeavour* pierced the clouds over Kennedy Space Center en route to the ISS.



Figure 32: Separation of the Solid Rocket Boosters.



Figure 33: *View of Endeavour (with cargo bay doors open) approaching the ISS.*

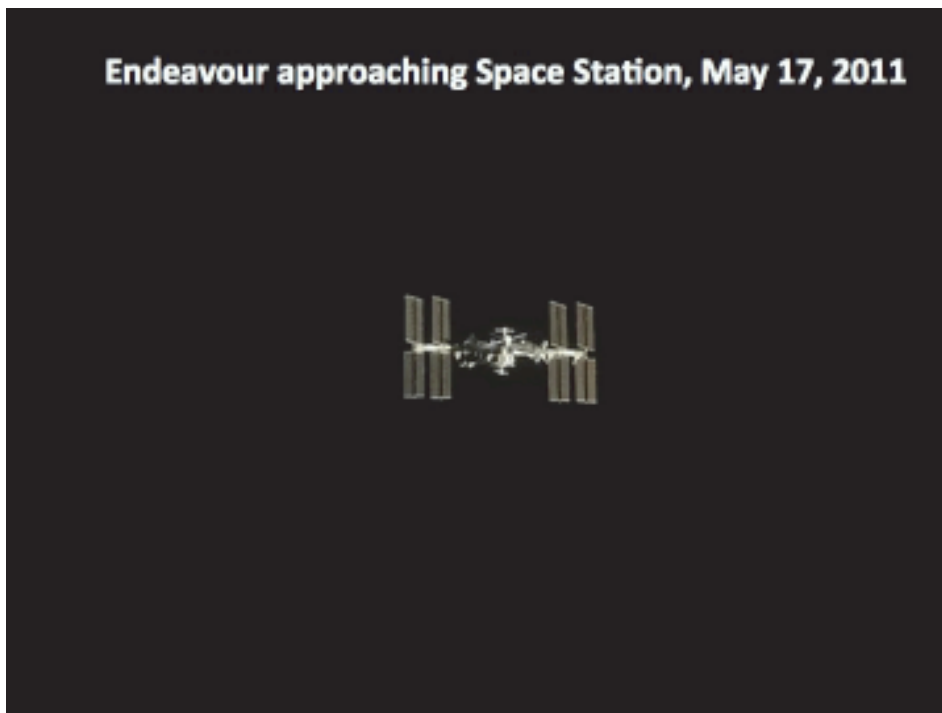




Figure 35: *View of the ISS through the flight deck windows of Endeavour during docking procedures*



Figure 36: *View of the ISS from Endeavour.*



Figure 37: After docking with the ISS, AMS was removed from *Endeavour's* cargo bay by the shuttle Remote Manipulator System and transferred to the ISS robotic arm that placed AMS on its permanent attachment site on an external truss of the ISS.



May 19: AMS installed on ISS 5:15 CDT, start taking data 9:35 CDT

During the first week, we collected 100 million cosmic rays

Figure 38: On May 19, 2011, AMS was deployed on the ISS. After three hours of checking all systems, AMS began to collect and transmit data to the AMS team on the ground.

After the launch, deployment and initial testing and commissioning of AMS on the ISS, the AMS team returned to CERN-Geneva. CERN had constructed a new building to house the main AMS Payload Operations Control Center (POCC) as seen in Figure 39. This facility was inaugurated on 19 June 2011. Since that time, AMS has been monitored and controlled by the AMS team working in close communication with NASA's ISS Control Center in Houston, Texas and Marshall Space Flight Center in Huntsville, Alabama.

AMS Control Center at CERN in control of AMS since 19 June 2011



Figure 39: *The interior of the main AMS Payload Operations Control Center (POCC) at CERN-Geneva. The main Science Operations Center (SOC) is also located at CERN-Geneva.*

AMS collected over 7 billion events

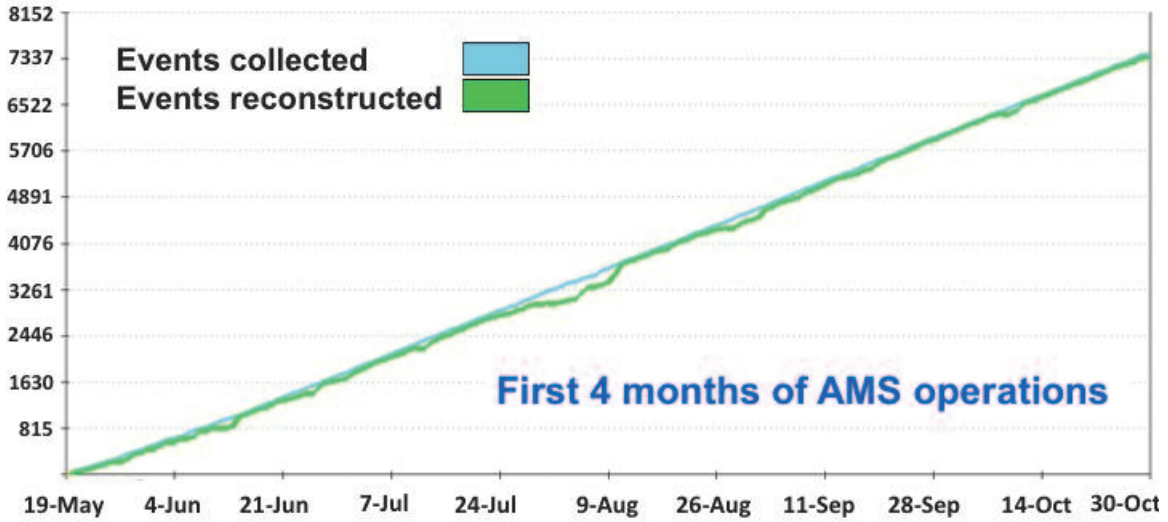


Figure 40: In the first four months of operations on the ISS, AMS collected and reconstructed over 7 billion cosmic ray events

In the first four months of operations, we have determined that the detectors function exactly as designed and have collected 7 billion events (see Figure 40). Therefore, every year, we will collect 1.5×10^{10} triggers and in 20 years we will collect 3×10^{11} triggers. This will provide unprecedented sensitivity to search for new physics. Figure 41 presents an example of the data from the first week.

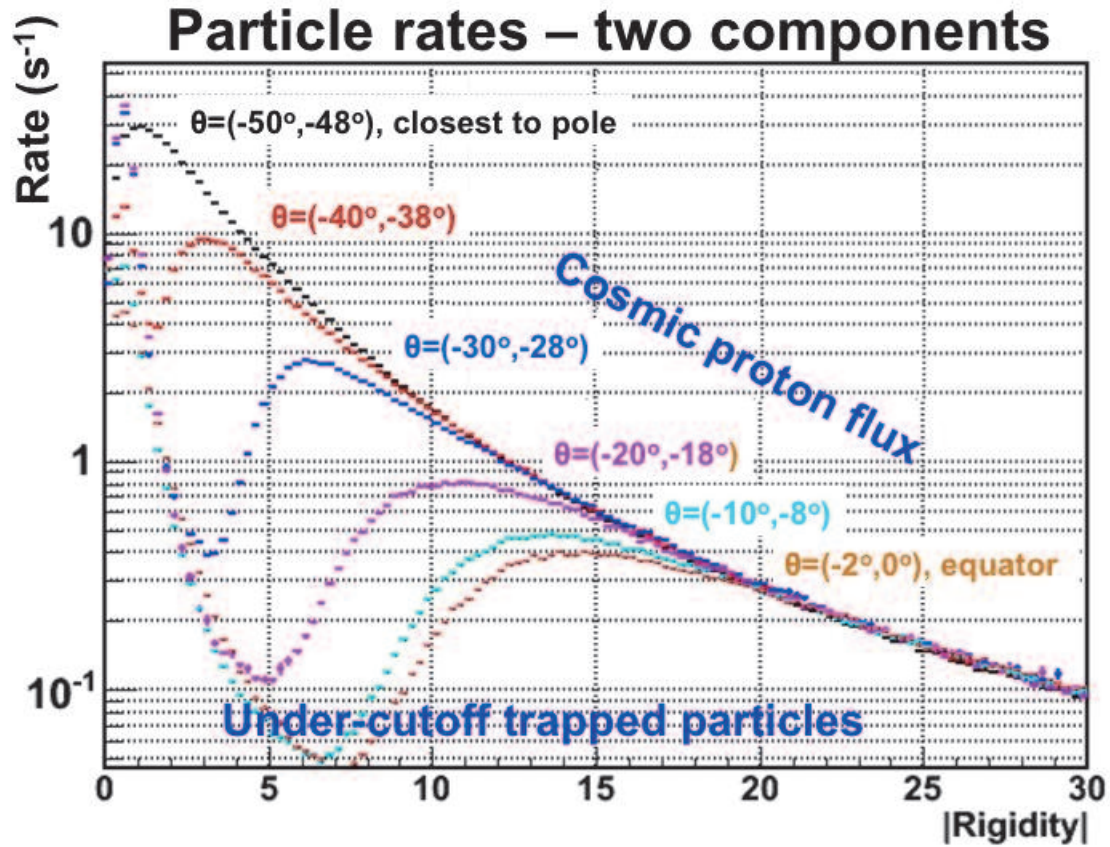


Figure 41: Cosmic proton flux of particles collected by AMS.

The physics objectives of AMS include the search for the origin of Dark Matter, the study of primary Cosmic Rays, the existence of Antimatter and to explore new phenomena, such as Strangelets.

Figures 42 through 51 present actual AMS data collected during the first three months of operation (19 May to 19 August 2011) as well as current theoretical models.

AMS Physics program example
Search for Cold Dark Matter

Many candidates from Particle Physics:

- SUSY neutralinos (χ^0)
- Kaluza-Klein bosons (B)
- ...

$\chi^0\chi^0 \rightarrow q\bar{q}, WW, ZZ, \gamma\gamma, l\bar{l} \rightarrow$ structures in the spectra of $e^+, \bar{p}, \bar{D}, \gamma$

J. Ellis et al., Phys. Lett. B, 214 (1988) 3
 M. Turner and F. Wilczek, Phys. Rev. D42 (1990) 4
 J. Ellis, CERN-PH-TH/2005-070

Figure 42: The search for the origin of Cold Dark Matter has several theoretical candidates such as SUSY neutralinos and Kaluza-Klein bosons, etc.

Indeed, the leading candidate for Dark Matter is the SUSY neutralino, as shown in Figure 43. AMS will be able to definitively identify the origin of Dark Matter through the excess in the spectra of e^+ in the collisions of X^0 , which is different from known cosmic ray collisions. Figure 44 shows AMS's ability to measure accurately the cosmic ray flux over the 11 year solar cycle from which the e^+ production from the collision of ordinary cosmic rays can be determined.

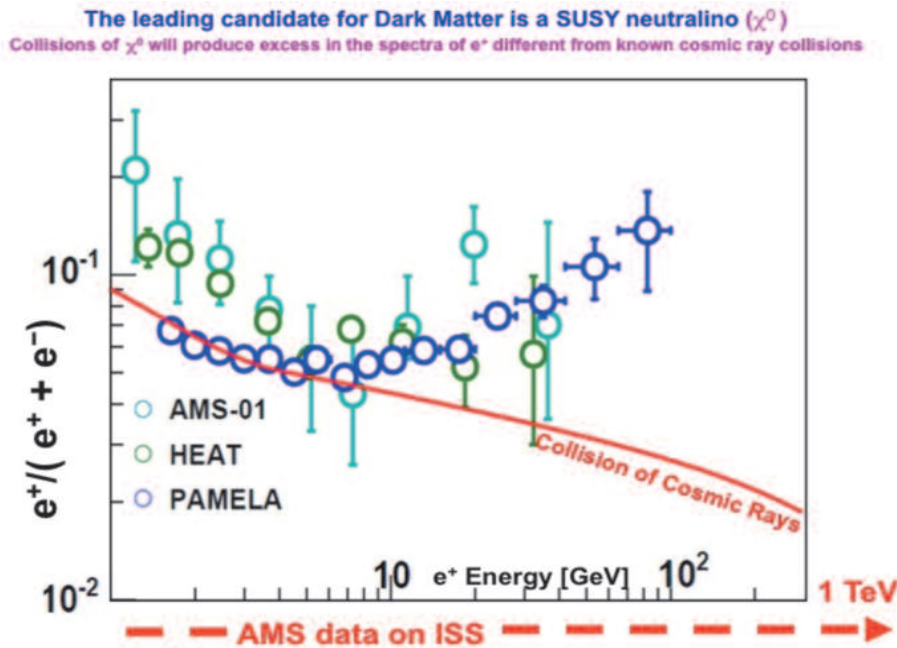
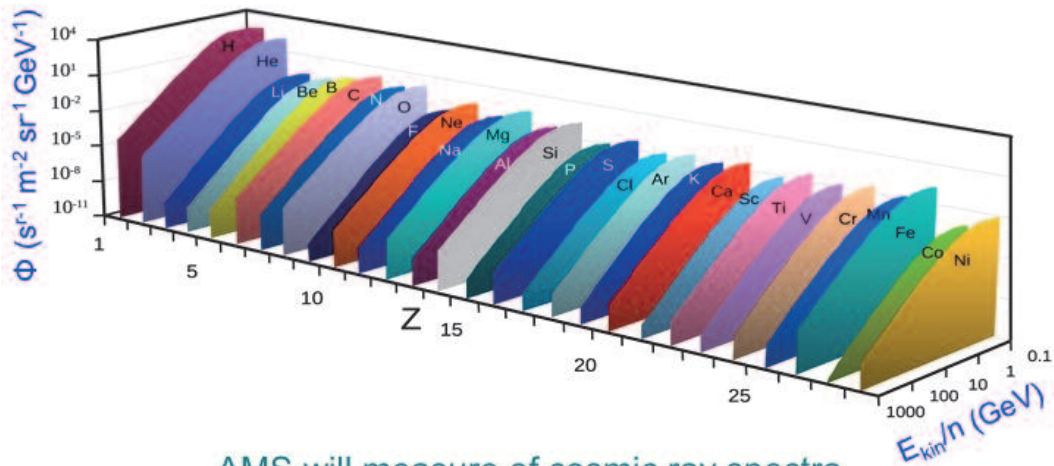


Figure 43: One of the leading theoretical candidates responsible for Dark Matter is the SUSY neutralino. AMS will be able to definitively identify the origin of Dark Matter through the excess in the spectra of e^+ in the collisions of X^0 , which is different from known cosmic ray collisions.

Physics of AMS: Nuclear Abundances Measurements



AMS will measure of cosmic ray spectra for nuclei, for energies from 100 MeV to 2 TeV with 1% accuracy over the 11-year solar cycle.

These spectra will provide experimental measurements of the assumptions that go into calculating the background in searching for Dark Matter, i.e., $p + C \rightarrow e^+, \bar{p}, \dots$

Figure 44: Data from AMS will be used to measure the cosmic ray spectra for nuclei for energies from 100 MeV to 2 TeV with unprecedented accuracy. This data will be applied to the calculation of background in the search for Dark Matter as noted above.

Figures 45 and 46 present Monte Carlo simulations of AMS data and current theoretical models. Figures 47 and 48 show 240 GeV electron events seen by AMS.

Detection of High Mass Dark Matter from ISS

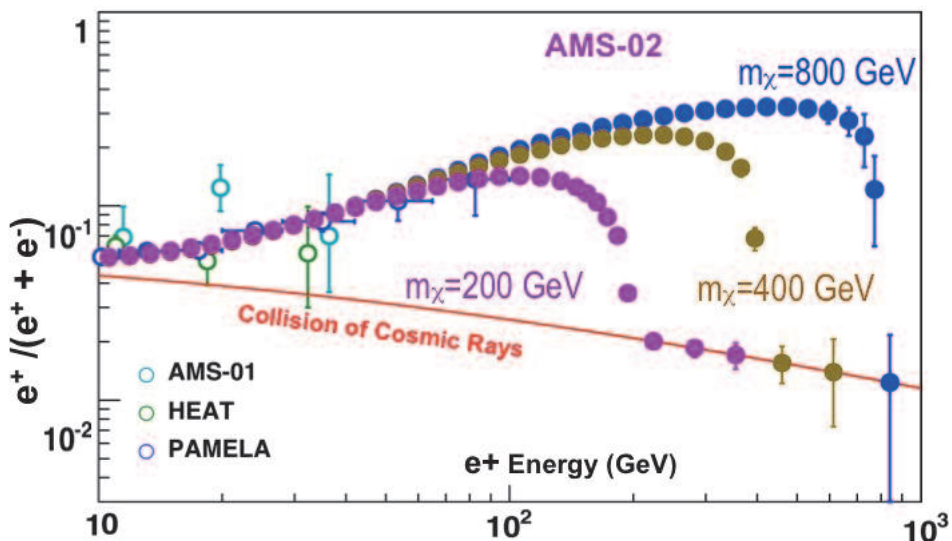
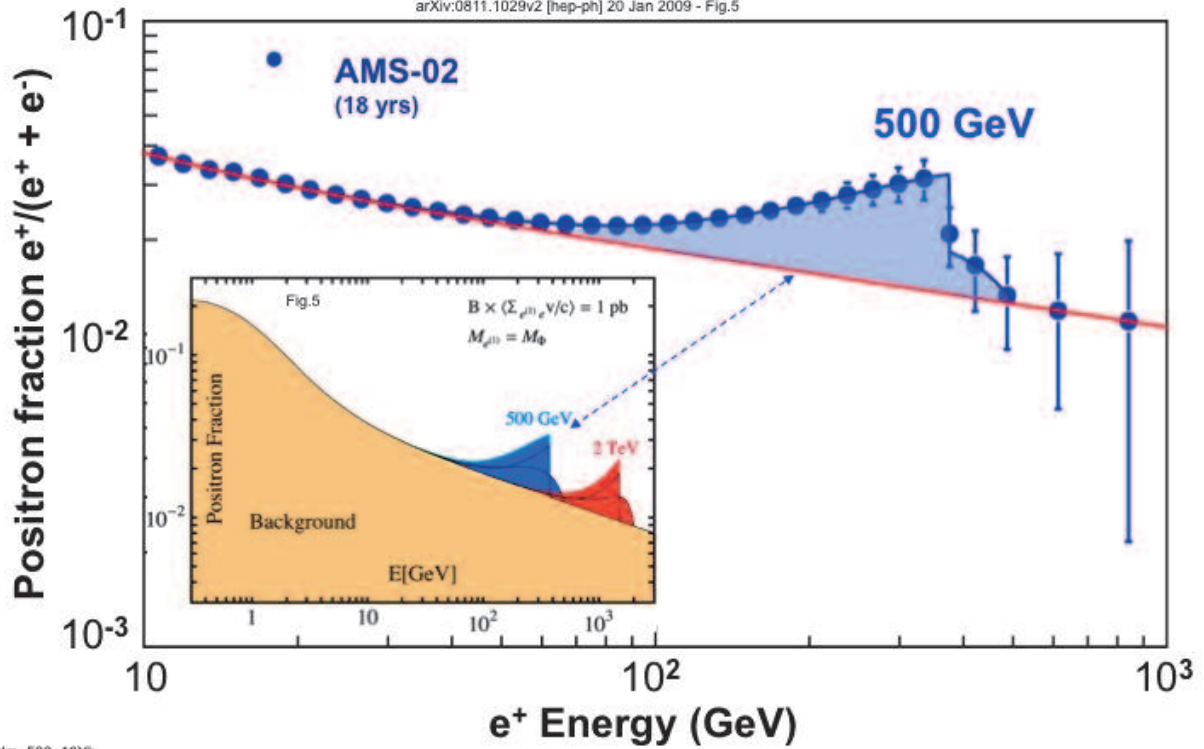


Figure 45: Comparison of Monte Carlo data for High Mass Dark Matter searches.

Kaluza-Klein Bosons are also Dark Matter candidates
case 2 TeV Scale Singlet Dark Matter

Eduardo Pontón and Lisa Randall

arXiv:0811.1029v2 [hep-ph] 20 Jan 2009 - Fig.5



sdm_500_18Yb

Figure 46: *In addition to the SUSY Neutralinos, the Kaluza-Klein Bosons are also theoretical candidates responsible for Dark Matter.*

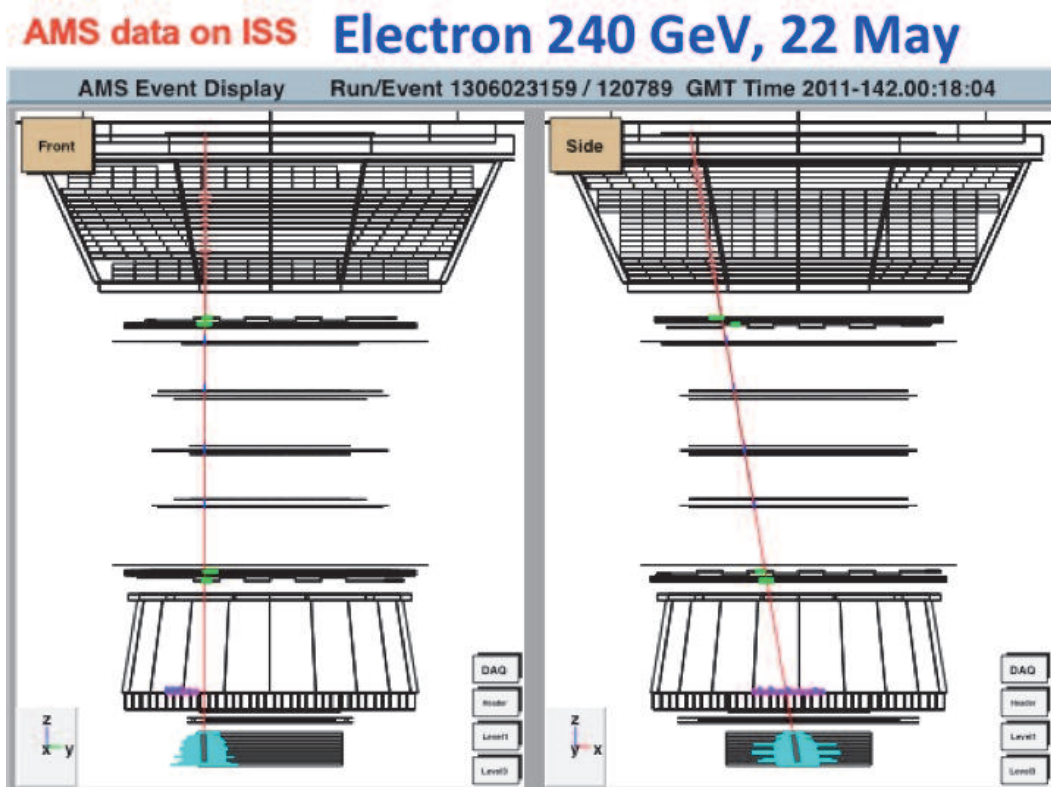


Figure 47: Actual event display from AMS on the ISS of a 240 GeV Electron.

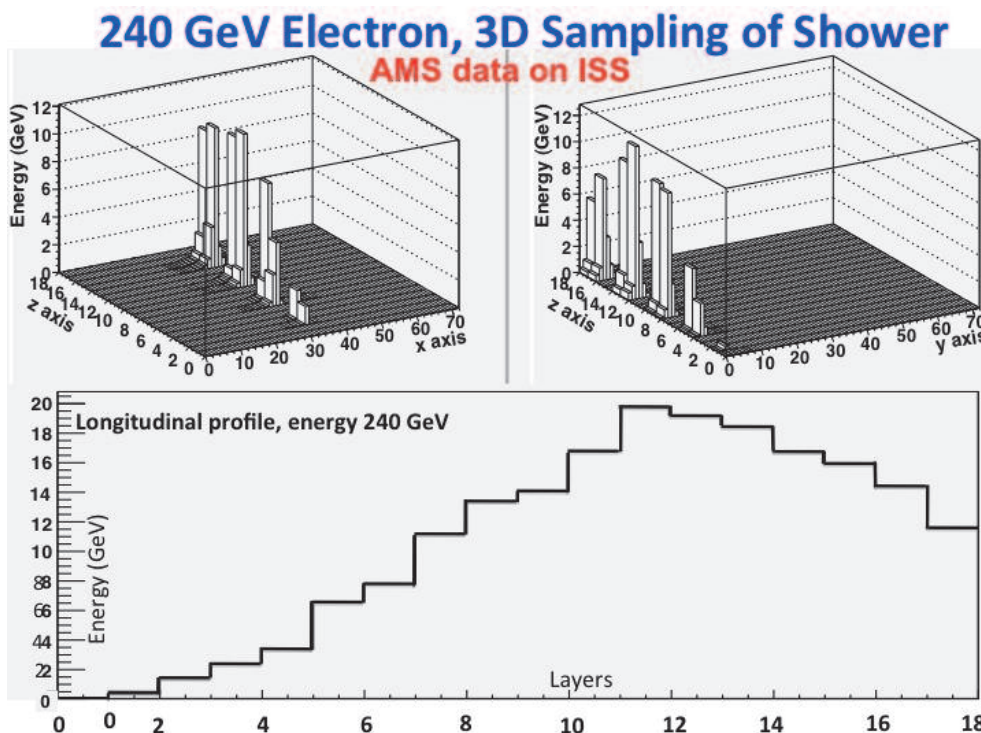


Figure 48: Actual data from AMS on the ISS of a 240 GeV Electron and 3D Sampling of Shower.

Another physics example of AMS is to search for Antimatter, the physics of which is illustrated in Figure 49.

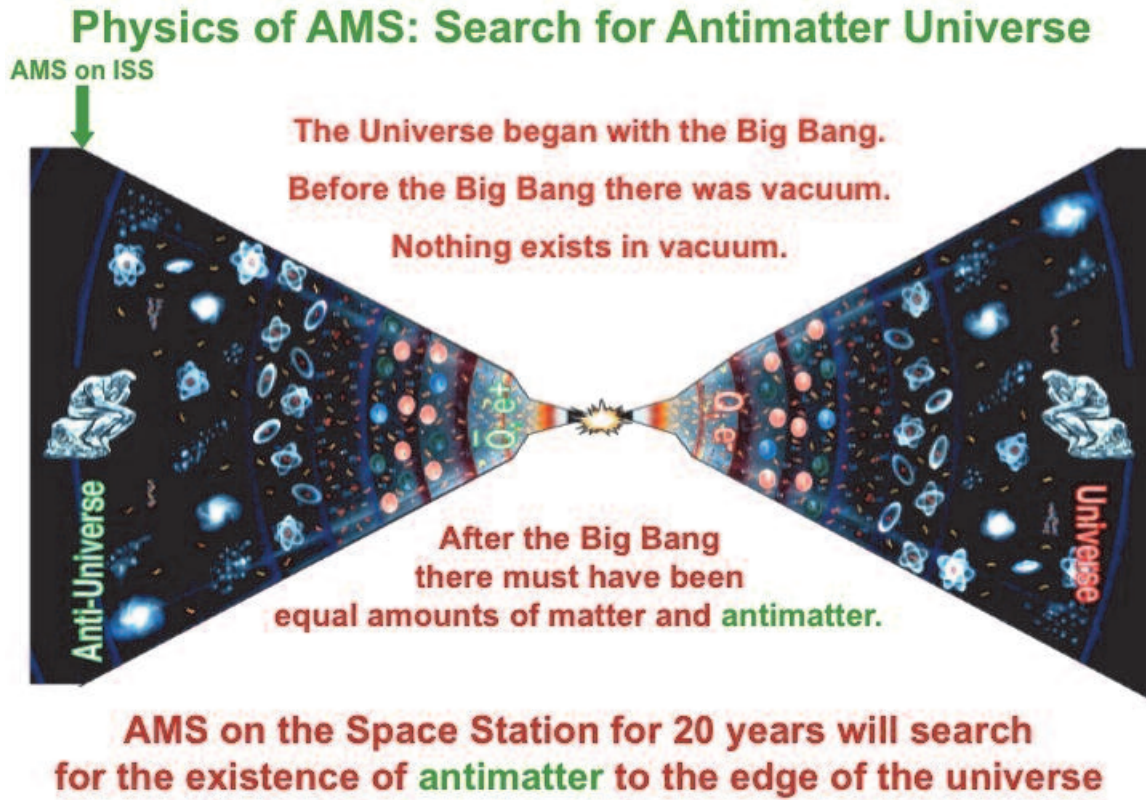


Figure 49: *The search for the Antimatter Universe is based on the Big Bang Theory of the Universe which states that equal amounts of matter and antimatter must have existed at the time of the Big Bang.*

AMS has often been referred to as the “Hubble Telescope for Charged Particles” since there has never before been a magnetic spectrometer in space for a long duration that could collect and study charged particles from primary sources in the far reaches of space before they enter the Earth’s atmosphere. Examples of current work on Antimatter are shown in Figure 50.

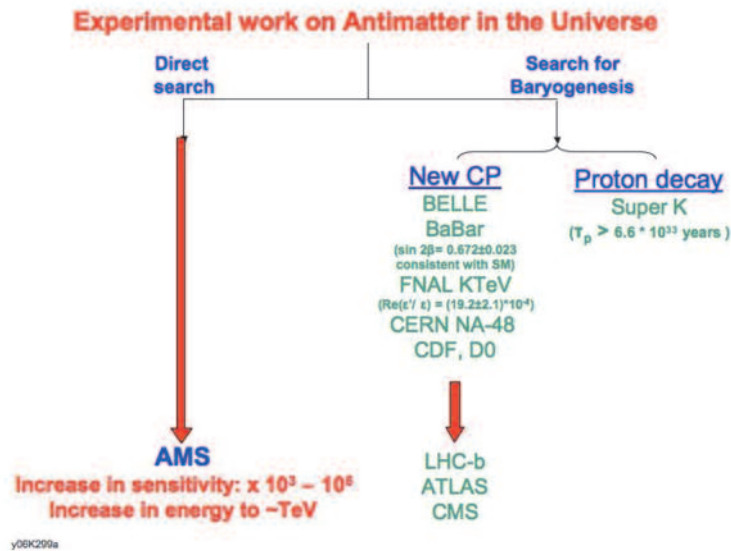


Figure 50: Current experimental work to search for Antimatter in the Universe is via the indirect search for Baryogenesis by new CP and Proton Decay, as represented by Belle, BaBar, FNAL, CERN the LHC experiments and by Super K. AMS is unique in that it is conducting a direct search for Antimatter.

Figure 51 shows an example of AMS’s ability to search for Antimatter and Figure 52 presents an example from the first three days of data measuring cosmic nuclei.

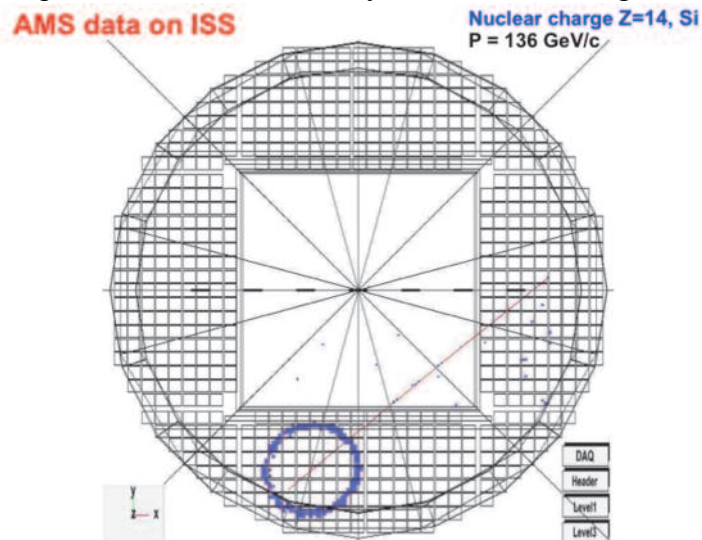


Figure 51: In order to ensure that an instrument can detect Antimatter, it must first detect Matter. This is illustrated above in the detection of Matter in the AMS RICH detector.

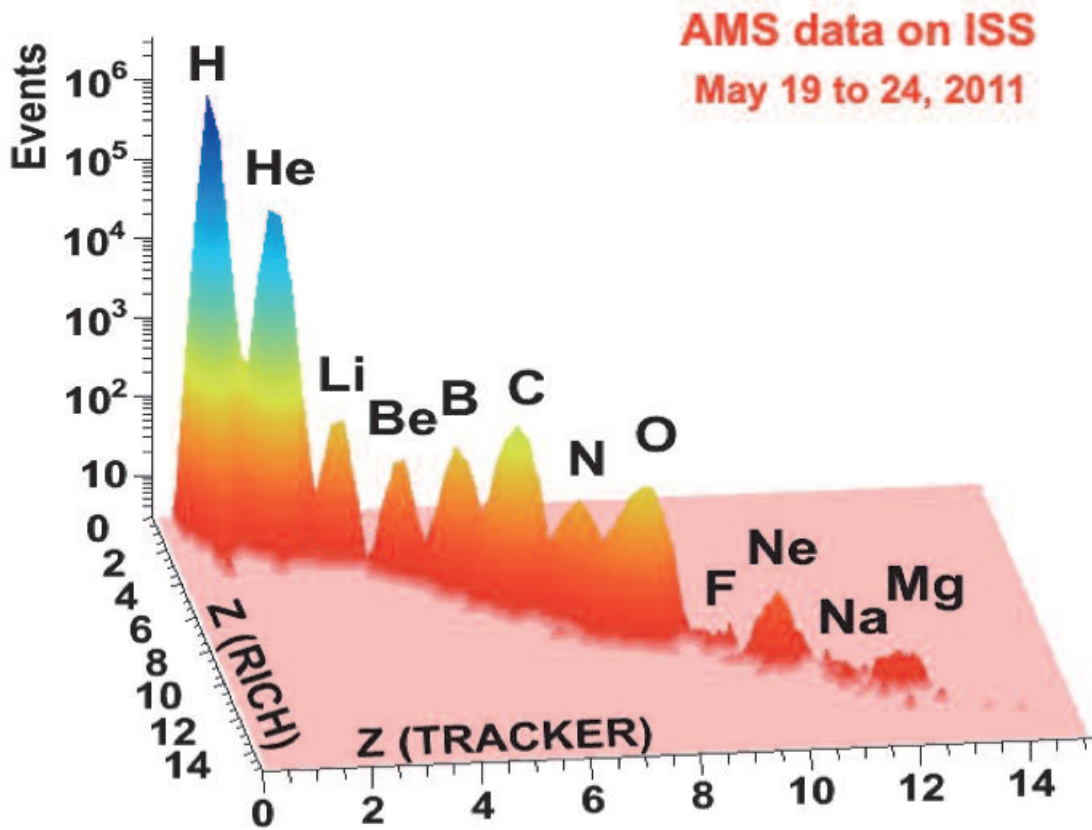
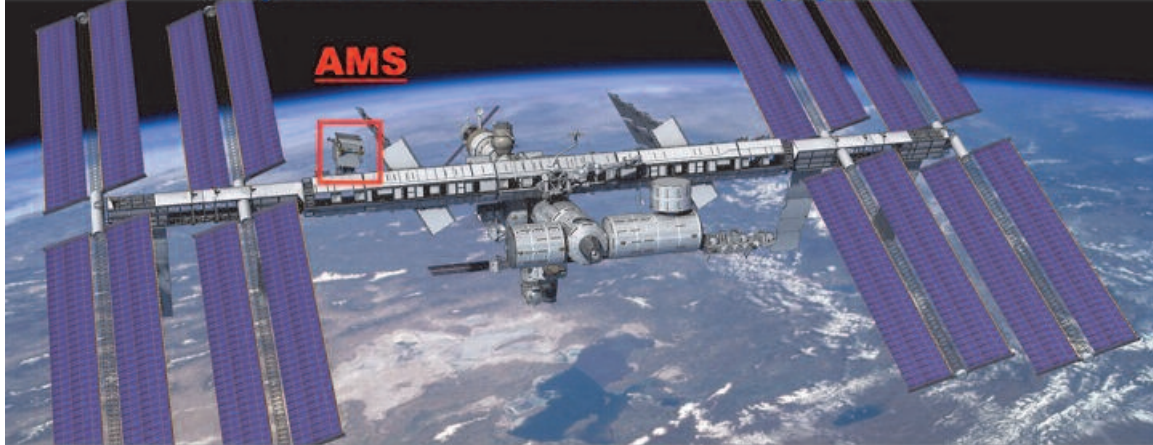


Figure 52: Data from the first week of AMS operations on the ISS. AMS will continue to collect nuclei to further expand the above spectra.

In conclusion, as illustrated in Figure 53, the cosmos is the ultimate laboratory, producing cosmic rays with energies far beyond what is possible to observe on Earth. AMS seeks to explore many of the fundamental questions in modern physics but the most important objective is to explore the unknown.

The Cosmos is the Ultimate Laboratory.
Cosmic rays can be observed at energies higher than any accelerator.

The issues of antimatter in the universe and the origin of Dark Matter probe the foundations of modern physics.



The most exciting objective of AMS is to probe the unknown; to search for phenomena which exist in nature that we have not yet imagined nor had the tools to discover.

Figure 53: *AMS on board the ISS will study the origin and structure of the cosmos which has the potential to make discoveries that will expand our reservoir of knowledge.*

However, discoveries in physics cannot be predicted in advance because objectives are always based on existing knowledge or “expert’s opinions”. As shown in Figure 54, most of the advances in physics were not originally the purpose of the facility or the experiment when approved. Advancements in our understanding of Nature and the Universe can only be made through experimental discoveries.

Discoveries in Physics

Facility	Original purpose, Expert Opinion	Discovery with Precision Instrument
P.S. CERN (1960's)	π N interactions	Neutral Currents -> Z, W
Brookhaven (1960's)	π N interactions	ν_e, ν_μ CP violation, J
FNAL (1970's)	Neutrino physics	b, t quarks
SLAC Spear (1970's)	ep, QED	Scaling, Ψ , τ
PETRA (1980's)	t quark	Gluon
Super Kamiokande (2000)	Proton decay	Neutrino oscillations
Hubble Space Telescope (1990's)	Galactic survey	Curvature of the universe, dark energy
AMS on ISS	Dark Matter, Antimatter Strangelets,...	?

Exploring a new territory with a precision instrument is the key to discovery.

y96402nac.ppt

Figure 54: Discoveries in physics compared to original purpose over the past fifty years.

Fundamental Science on the International Space Station

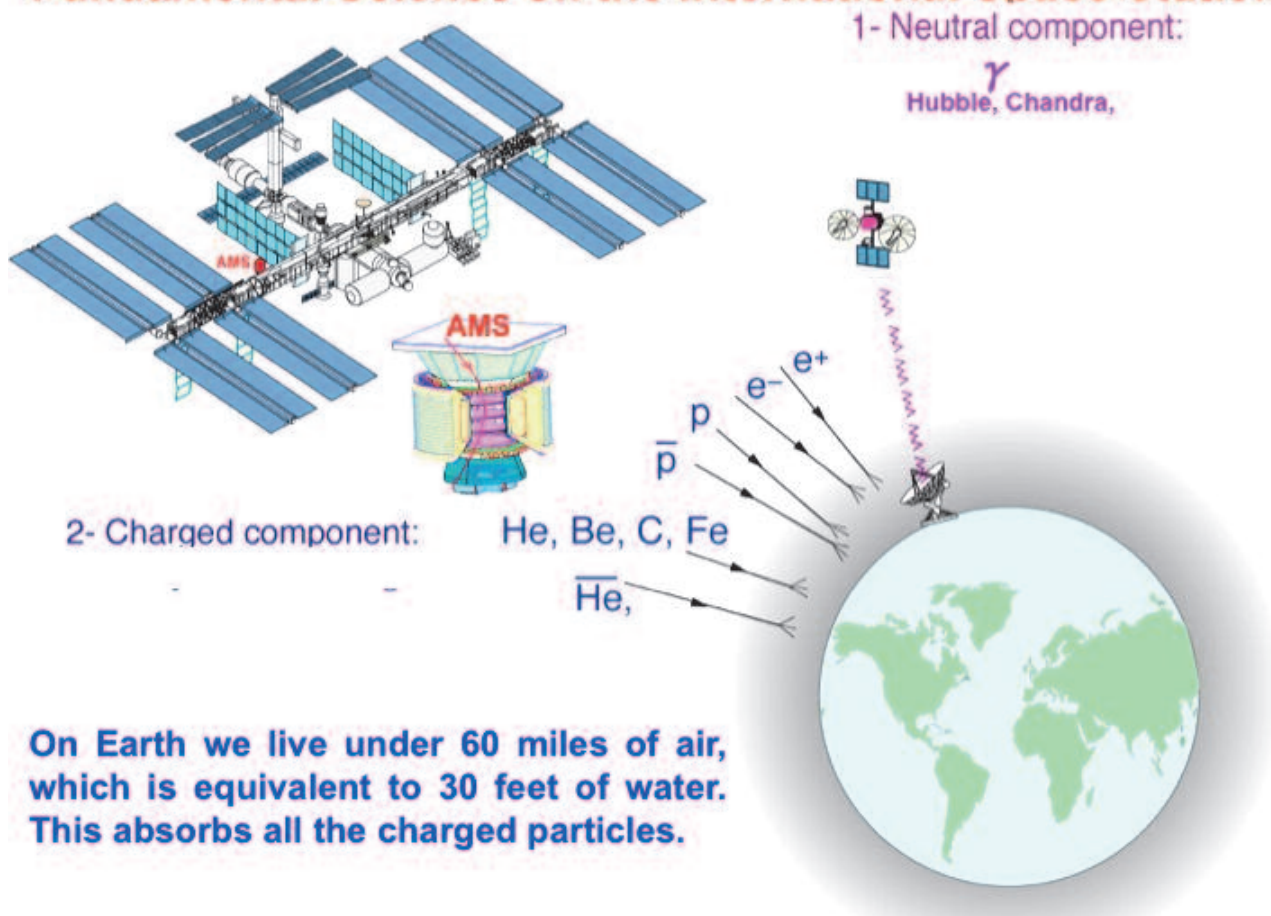


Figure 55: *The International Space Station provides a unique opportunity to support fundamental science above the Earth's atmosphere.*

As seen in Figure 55, fundamental physics on the International Space Station has the potential to yield important information impossible to attain on the ground or with short duration balloon experiments. AMS will thus explore a new domain in particle physics research.